Gutzwiller wave function on a quantum computer using a discrete Hubbard-Stratonovich transformation

Kazuhiro Seki,[1] Yuichi Otsuka,[1, 2] and Seiji Yunoki[1, 2, 3, 4]

[1]*Quantum Computational Science Research Team, RIKEN Center for Quantum Computing (RQC), Saitama 351-0198, Japan*
[2]*Computational Materials Science Research Team, RIKEN Center for Computational Science (R-CCS), Hyogo 650-0047, Japan*
[3]*Computational Quantum Matter Research Team, RIKEN Center for Emergent Matter Science (CEMS), Saitama 351-0198, Japan*
[4]*Computational Condensed Matter Physics Laboratory,*
RIKEN Cluster for Pioneering Research (CPR), Saitama 351-0198, Japan
(Dated: April 15, 2022)

We propose a quantum-classical hybrid scheme for implementing the nonunitary Gutzwiller factor using a discrete Hubbard-Stratonovich transformation, which allows us to express the Gutzwiller factor as a linear combination of unitary operators involving only single-qubit rotations, at the cost of the sum over the auxiliary fields. To perform the sum over the auxiliary fields, we introduce two approaches that have complementary features. The first approach employs a linear-combination-of-unitaries circuit, which enables one to probabilistically prepare the Gutzwiller wave function on a quantum computer, while the second approach uses importance sampling to estimate observables stochastically, similar to a quantum Monte Carlo method in classical computation. The proposed scheme is demonstrated with numerical simulations for the half-filled Fermi-Hubbard model. Furthermore, we perform quantum simulations using a real quantum device, demonstrating that the proposed scheme can reproduce the exact ground-state energy of the two-site Fermi-Hubbard model within error bars.

I. INTRODUCTION

Solving quantum many-body systems directly using classical computers requires exponentially large computational resources that are often beyond the feasibility of current high-performance computing facilities. To overcome this difficulty, at least in part, a tremendous amount of effort has been devoted so far and several theoretical and numerical techniques have been successfully developed [1]. It should also be pointed out that, as one of the next-generation computing paradigms, quantum computing [2] has attracted growing interest for solving quantum many-body systems, which is becoming realistic, evidenced by the recent technological advances [3–12]. In this regards, the variational-quantum-eigensolver method and its variants have been proposed and demonstrated for computing ground-state [13–23] and low-lying excited-state [24–29] properties of quantum-many-body systems by exploiting noisy intermediate-scale quantum (NISQ) [30] computers and classical computers in a hybrid manner. For recent reviews on variational quantum algorithms, see for example Refs. [31–34]. It is also remarkable that physically motivated wave function such as Gutzwiller- and Jastrow-type wave functions [20] and a resonating-valence-bond-type wave function [35] have been implemented with NISQ computers.

The Gutzwiller wave function is known as a variational state for quantum-many-body systems in condensed matter physics that allows us to take into account electron correlation effects beyond the level of a single Slater-determinant state [36]. Despite its formal simplicity, the Gutzwiller-type wave functions, including Gutzwiller-projected Fermi-sea states [37], Gutzwiller-projected BCS states [38, 39], and Gutzwiller-projected Hartree-Fock states [40], can describe ground and low-lying excited states of several quantum many-body systems such as a lattice model of dimers [41], the Haldane-Shastry model [42, 43], and t-J-type models [44–50]

(for a recent ground-state phase diagram of the t-t'-J model using the density-matrix-renormalization-group method, see Ref. [51]) qualitatively or even exactly in some particular cases.

In classical computation, the Gutzwiller wave function can be implemented rather straightforwardly when the Gutzwiller factor is diagonal in a computational basis. In quantum computation, one can also choose the computational basis states so that the Gutzwiller factor is diagonal. However, implementing a Gutzwiller-type wave function on a quantum computer is not straightforward due to its nonunitarity, and several schemes for implementing it have been developed [20, 52, 53]. Mazzola *et al.* [20] evaluates the expectation value of energy with respect to a Jastrow-type wave function [54, 55] by measuring the transformed Hamiltonian $\hat{P}_{\mathrm{J}}\hat{\mathcal{H}}\hat{P}_{\mathrm{J}}$ and the squared Jastrow factor $(\hat{P}_{\mathrm{J}})^2$ with a suitably truncated expansion of the Jastrow factor $\hat{P}_{\mathrm{J}}$. Murta and Fernández-Rossier [53] proposed a quantum circuit for probabilistically preparing the Gutzwiller wave function using ancillary qubits. It is also noteworthy that, aside from the Gutzwiller wave function, general frameworks for probabilistically performing nonunitary operations on a quantum computer have been proposed [56–58].

In this paper, we propose another scheme for implementing the Gutzwiller wave function using a discrete version [59] of the Hubbard-Stratonovich transformation [60], which allows us to represent the Gutzwiller factor as a linear combination of unitary operators, at the expense of introducing the auxiliary fields. In order to sum all the auxiliary fields, we introduce two different but complimentary approaches based on (i) a quantum circuit for the linear combination of unitary operators and (ii) an importance sampling technique. Furthermore, the proposed scheme is demonstrated using numerical simulations as well as a real quantum device.

The rest of this paper is organized as follows. In Sec. II, we provide formalism of the proposed scheme. We first define the Hamiltonian of the Fermi-Hubbard model and the Gutzwiller wave function. Then we describe the discrete Hubbard-

Stratonovich transformation for the Gutzwiller factor, and introduce the Jordan-Wigner transformation to construct concrete quantum circuits for implementing the Gutzwiller wave function on a quantum computer. In Sec. III, we describe two complementary approaches for performing the sum over the auxiliary fields. The first approach employs a linear-combination-of-unitaries circuit for probabilistically preparing the Gutzwiller wave function on a quantum computer. The second approaches uses an importance sampling technique to stochastically evaluate observables with respect to the Gutzwiller wave function. We also describe a simplification scheme that is applicable when the trial state is a separable state with respect to the spin degrees of freedom. The two approaches are demonstrated by numerical simulations for the Fermi-Hubbard model up to 12 sites. In Sec. IV, we apply the proposed scheme for calculating ground-state properties of the two-site Fermi-Hubbard model at half filling by using a NISQ computer. First, we summarize the Gutzwiller wave function approach for the ground-state of two-site Fermi-Hubbard model at half filling, where the Gutzwiller wave function can describe the ground state exactly. Then we show the results obtained by using a NISQ computer. Conclusions and discussions are given in Sec. V. In Appendix A, we provide a general scheme for finding discrete Hubbard-Stratonovich transformations, which decompose an exponentiated density-density interaction term into a linear combination of two-qubit unitary operators. In Appendix B, we prove the absence of the phase problem in the second approach for the Fermi-Hubbard model on a bipartite lattice at half filling.

II. MODEL AND FORMALISM

A. Fermi-Hubbard model

We consider the Fermi-Hubbard model defined by the Hamiltonian

$$\hat{\mathcal{H}} = \hat{K} + U\hat{D}, \qquad (1)$$

where

$$\hat{K} = -J \sum_{\sigma=\uparrow,\downarrow} \sum_{\langle i,j \rangle} \left(\hat{c}_{i\sigma}^\dagger \hat{c}_{j\sigma} + \text{H.c.} \right) \qquad (2)$$

and

$$\hat{D} = \sum_{i=1}^{N_{\text{site}}} \left(\hat{n}_{i\uparrow} - \tfrac{1}{2} \right)\left(\hat{n}_{i\downarrow} - \tfrac{1}{2} \right). \qquad (3)$$

Here, J is the hopping parameter, U is the interaction parameter, N_{site} is the number of sites, and $\hat{c}_{i\sigma}^\dagger$ ($\hat{c}_{i\sigma}$) is the creation (annihilation) operator of a fermion at site $i\,(= 1, 2, \cdots, N_{\text{site}})$ with spin $\sigma\,(=\uparrow,\downarrow)$. The summation $\sum_{\langle i,j \rangle} \cdots$ denotes the sum over all pairs of nearest-neighbor sites i and j. $\hat{n}_{i\sigma} = \hat{c}_{i\sigma}^\dagger \hat{c}_{i\sigma}$ is the fermion number operator at site i with spin σ. In this study, we assume $J > 0$ and $U \geqslant 0$.

B. Gutzwiller wave function

The Gutzwiller wave function

$$|\psi_g\rangle \equiv \frac{\mathrm{e}^{-g\hat{D}}|\psi_0\rangle}{\sqrt{\langle\psi_0|\mathrm{e}^{-2g\hat{D}}|\psi_0\rangle}}, \qquad (4)$$

is known as a variational state for the Fermi-Hubbard model [36]. Here, $\mathrm{e}^{-g\hat{D}}$ is the Gutzwiller factor with $0 \leqslant g < \infty$ being the dimensionless variational parameter that penalizes the double occupancy of fermions at the same site, and $|\psi_0\rangle$ is a trial state. In this study, we assume that $|\psi_0\rangle$ is normalized as $\langle\psi_0|\psi_0\rangle = 1$ and it is an eigenstate of the total particle-number operator $\hat{N} \equiv \sum_i \sum_\sigma \hat{n}_{i\sigma}$. Since $[\hat{N}, \hat{D}] \equiv \hat{N}\hat{D} - \hat{D}\hat{N} = 0$, $|\psi_g\rangle$ is also an eigenstate of $\hat{N}$. Typically, the trial state $|\psi_0\rangle$ is chosen as a single Slater-determinant state such as the ground state of $\hat{K}$ or a single-particle mean-field Hamiltonian. The Gutzwiller wave function $|\psi_g\rangle$ can take into account electron correlation effects beyond the trial state $|\psi_0\rangle$.

There is one remark on the Gutzwiller factor. Originally, the Gutzwiller factor was introduced in the following form [36]

$$\hat{G}(\tilde{g}) \equiv \prod_{i=1}^{N_{\text{site}}} \left[1 - (1 - \tilde{g})\hat{n}_{i\uparrow}\hat{n}_{i\downarrow} \right] \overset{\tilde{g}\neq 0}{=} \tilde{g}^{\sum_i \hat{n}_{i\uparrow}\hat{n}_{i\downarrow}}, \qquad (5)$$

where $0 \leqslant \tilde{g} \leqslant 1$ is the variational parameter and the right-hand side is valid for $\tilde{g} \neq 0$. If $\tilde{g} = 0$, $\hat{G}(0) = \prod_{i=1}^{N_{\text{site}}}(1 - \hat{n}_{i\uparrow}\hat{n}_{i\downarrow})$, which excludes fermion configurations with doubly occupied sites from $|\psi_0\rangle$, and $\hat{G}(0)$ is called the Gutzwiller projector [61]. Provided that $|\psi_0\rangle$ is an eigenstate of the total particle-number operator $\hat{N}$, we can easily show that the following equality holds:

$$|\psi_g\rangle = \frac{\mathrm{e}^{-g\hat{D}}|\psi_0\rangle}{\sqrt{\langle\psi_0|\mathrm{e}^{-2g\hat{D}}|\psi_0\rangle}} = \frac{\hat{G}(\tilde{g})|\psi_0\rangle}{\sqrt{\langle\psi_0|\hat{G}(\tilde{g})^2|\psi_0\rangle}} \qquad (6)$$

with the parameters $\tilde{g}$ and g satisfying the relation (see, e.g., Ref. [62])

$$\tilde{g} = \mathrm{e}^{-g}. \qquad (7)$$

Therefore, using $\mathrm{e}^{-g\hat{D}}$ is equivalent to using $\hat{G}(\tilde{g})$ for expressing the Gutzwiller wave function $|\psi_g\rangle$, despite that $\mathrm{e}^{-g\hat{D}} \neq \hat{G}(\tilde{g})$. The reason why we use $\mathrm{e}^{-g\hat{D}}$ is simply because $\mathrm{e}^{-g\hat{D}}$ is readily compatible with the Hubbard-Stratonovich transformation, as described in the next section.

C. Discrete Hubbard-Stratonovich transformation

To express the Gutzwiller factor $\mathrm{e}^{-g\hat{D}}$ as a linear combination of unitary operators, we introduce the discrete Hubbard-Stratonovich transformation [59]

$$\mathrm{e}^{-g\left(\hat{n}_{i\uparrow} - \frac{1}{2}\right)\left(\hat{n}_{i\downarrow} - \frac{1}{2}\right)} = \gamma \sum_{s_i=\pm 1} \mathrm{e}^{\mathrm{i}\alpha s_i(\hat{n}_{i\uparrow} + \hat{n}_{i\downarrow} - 1)}, \qquad (8)$$

where $s_i (= \pm 1)$ is the discrete auxiliary field, $\gamma = \mathrm{e}^{g/4}/2$, and

$$\alpha = \arccos\left(\mathrm{e}^{-g/2}\right). \tag{9}$$

Since the fermion number operators commute with each other, $[\hat{n}_{i\sigma}, \hat{n}_{j\sigma'}] = 0$, the Gutzwiller factor can be written simply as

$$\mathrm{e}^{-g\hat{D}} = \gamma^{N_{\mathrm{site}}} \prod_{i=1}^{N_{\mathrm{site}}} \sum_{s_i=\pm 1} \mathrm{e}^{2\mathrm{i}\alpha s_i \hat{\eta}_i^z} \tag{10}$$

$$= \gamma^{N_{\mathrm{site}}} \prod_{i=1}^{N_{\mathrm{site}}} \left(\mathrm{e}^{2\mathrm{i}\alpha\hat{\eta}_i^z} + \mathrm{e}^{-2\mathrm{i}\alpha\hat{\eta}_i^z}\right), \tag{11}$$

where

$$\hat{\eta}_i^z \equiv \frac{1}{2}\left(\hat{n}_{i\uparrow} + \hat{n}_{i\downarrow} - 1\right) \tag{12}$$

is introduced to simplify the notation. Now the nonunitary Gutzwiller factor [left-hand side of Eq. (11)] is expressed as a linear combination of unitary operators [right-hand side of Eq. (11)] after summing all the auxiliary fields $\{s_i\}_{i=1}^{N_{\mathrm{site}}}$. The different decomposition schemes of the Hubbard-Stratonovich transformation that are potentially useful for other purposes are provided in Appendix A.

The expectation value of an operator $\hat{O}$ with respect to the Gutzwiller wave function $|\psi_g\rangle$ is given by

$$\langle\hat{O}\rangle \equiv \langle\psi_g|\hat{O}|\psi_g\rangle = \frac{\langle\psi_0|\mathrm{e}^{-g\hat{D}}\hat{O}\mathrm{e}^{-g\hat{D}}|\psi_0\rangle}{\langle\psi_0|\mathrm{e}^{-2g\hat{D}}|\psi_0\rangle} \tag{13}$$

$$= \frac{\sum_s \langle\psi_0|\prod_{i=1}^{N_{\mathrm{site}}}\mathrm{e}^{2\mathrm{i}\alpha s_{i,2}\hat{\eta}_i^z}\hat{O}\prod_{j=1}^{N_{\mathrm{site}}}\mathrm{e}^{2\mathrm{i}\alpha s_{j,1}\hat{\eta}_j^z}|\psi_0\rangle}{\sum_{s'}\langle\psi_0|\prod_{i=1}^{N_{\mathrm{site}}}\mathrm{e}^{2\mathrm{i}\alpha(s'_{i,1}+s'_{i,2})\hat{\eta}_i^z}|\psi_0\rangle}, \tag{14}$$

where

$$\sum_s \cdots \equiv \prod_{\tau=1}^{N_\tau}\prod_{i=1}^{N_{\mathrm{sites}}}\sum_{s_{i,\tau}=\pm 1}\cdots \tag{15}$$

represents the sum over the auxiliary fields $\{\{s_{i,\tau} = \pm 1\}_{i=1}^{N_{\mathrm{site}}}\}_{\tau=1}^{N_\tau}$ with $N_\tau = 2$, implying that the total number of terms in the sum over s is $2^{N_\tau \cdot N_{\mathrm{site}}} = 4^{N_{\mathrm{site}}}$. Notice that another label $\tau (= 1, 2)$ for the auxiliary fields is introduced to distinguish the auxiliary fields corresponding to the bra and ket states, i.e., $\tau = 1$ for $\langle\psi_g|$ and $\tau = 2$ for $|\psi_g\rangle$ [63].

D. Jordan-Wigner transformation

The formalism described above is given in terms of the fermion operators. In order to implement the proposed scheme on a quantum computer, we now apply the Jordan-Wigner transformation of the form

$$\hat{c}_{i\sigma}^\dagger \overset{\mathrm{JWT}}{=} \frac{1}{2}(\hat{X}_{i_\sigma} - \mathrm{i}\hat{Y}_{i_\sigma})\prod_{k<i_\sigma}\hat{Z}_k \tag{16}$$

and

$$\hat{c}_{i\sigma} \overset{\mathrm{JWT}}{=} \frac{1}{2}(\hat{X}_{i_\sigma} + \mathrm{i}\hat{Y}_{i_\sigma})\prod_{k<i_\sigma}\hat{Z}_k, \tag{17}$$

where $i_\sigma (= 1, 2, \cdots, 2N_{\mathrm{site}})$ is the one-dimensional label for the site and spin indexes and $\hat{X}_{i_\sigma}$, $\hat{Y}_{i_\sigma}$, and $\hat{Z}_{i_\sigma}$ are Pauli X, Y, and Z operators acting on the i_σth qubit. By $\cdots \overset{\mathrm{JWT}}{=} \cdots$ in Eqs. (16) and (17), we denote that the fermion operators on the left-hand side are expressed in terms of the Pauli operators under the Jordan-Wigner transformation.

Using the Jordan-Wigner transformation, the kinetic term in Eq. (2) and the interaction term in Eq. (3) of the Hamiltonian can be expressed with the Pauli operators as

$$\hat{K} \overset{\mathrm{JWT}}{=} -\frac{J}{2}\sum_\sigma\sum_{\langle i_\sigma, j_\sigma\rangle}\left(\hat{X}_{i_\sigma}\hat{X}_{j_\sigma} + \hat{Y}_{i_\sigma}\hat{Y}_{j_\sigma}\right)\hat{Z}_{\mathrm{JW},i_\sigma j_\sigma} \tag{18}$$

and

$$\hat{D} \overset{\mathrm{JWT}}{=} \frac{1}{4}\sum_{i=1}^{N_{\mathrm{site}}}\hat{Z}_{i_\uparrow}\hat{Z}_{i_\downarrow}, \tag{19}$$

respectively, where $\hat{Z}_{\mathrm{JW},ij} = \prod_{i\leqslant k\leqslant j}\hat{Z}_k$ is the Jordan-Wigner string for $i \leqslant k \leqslant j$ and $\hat{Z}_{\mathrm{JW},ij} = \hat{I}$ (identity operator) for $i = j \pm 1$. Similarly, the operator $\hat{\eta}_i^z$ in Eq. (12) can be expressed as

$$\hat{\eta}_i^z \overset{\mathrm{JWT}}{=} -\frac{1}{4}\left(\hat{Z}_{i_\uparrow} + \hat{Z}_{i_\downarrow}\right) \doteq \frac{1}{2}\begin{bmatrix} -1 & 0 & 0 & 0 \\ 0 & 0 & 0 & 0 \\ 0 & 0 & 0 & 0 \\ 0 & 0 & 0 & 1 \end{bmatrix}, \tag{20}$$

where $\doteq$ indicates the matrix representation and the matrix here is represented with the computational basis states $|00\rangle \equiv |0\rangle_{i_\uparrow}|0\rangle_{i_\downarrow}$, $|01\rangle \equiv |0\rangle_{i_\uparrow}|1\rangle_{i_\downarrow}$, $|10\rangle \equiv |1\rangle_{i_\uparrow}|0\rangle_{i_\downarrow}$, and $|11\rangle \equiv |1\rangle_{i_\uparrow}|1\rangle_{i_\downarrow}$ with $\hat{Z}_{i_\sigma}|0\rangle_{i_\sigma} = |0\rangle_{i_\sigma}$ and $\hat{Z}_{i_\sigma}|1\rangle_{i_\sigma} = -|1\rangle_{i_\sigma}$. Finally, the rotation generated by $2\hat{\eta}_i^z$ can be expressed as a product of the one-qubit rotations, i.e.,

$$\mathrm{e}^{2\mathrm{i}\alpha\hat{\eta}_i^z} \overset{\mathrm{JWT}}{=} \hat{R}_{Z_{i_\uparrow}}(\alpha) \otimes \hat{R}_{Z_{i_\downarrow}}(\alpha) \doteq \begin{bmatrix} \mathrm{e}^{-\mathrm{i}\alpha} & 0 & 0 & 0 \\ 0 & 1 & 0 & 0 \\ 0 & 0 & 1 & 0 \\ 0 & 0 & 0 & \mathrm{e}^{\mathrm{i}\alpha} \end{bmatrix}, \tag{21}$$

where

$$\hat{R}_Z(\alpha) = \exp\left(-\mathrm{i}\alpha\hat{Z}/2\right). \tag{22}$$

Notice that $\mathrm{e}^{2\mathrm{i}\alpha\hat{\eta}_i^z}$ acts nontrivially only on the empty state (corresponding to $|00\rangle$) and the doubly occupied state (corresponding to $|11\rangle$). Equation (21) shows that, under the Jordan-Wigner transformation, $\mathrm{e}^{2\mathrm{i}\alpha\hat{\eta}_i^z}$ is expressed simply as a direct product of the single-qubit Z rotation gates with the same rotation angle α.

III. SUM OVER AUXILIARY FIELDS

Since the terms involved in the sum over the auxiliary fields in Eqs. (10) and (14) increases exponentially in N_{site}, performing directly the sum becomes unfeasible as N_{site} is large. Nevertheless, here we introduce two approaches, based on (i) a

quantum circuit for a linear combination of unitary operators and (ii) an importance sampling technique, for performing the sum over the auxiliary fields. These two approaches have complementary features.

The first approach based on a quantum circuit for a linear combination of unitary operators allows us to probabilistically prepare the Gutzwiller wave function $|\psi_g\rangle$ on a quantum computer by using N_{site} ancillary qubits, which can be trivially reduced to one if an ancillary qubit is reused, and $2N_{\text{site}}$ controlled-R_Z operations. However, the probability for successfully preparing the desired state decreases exponentially in N_{site}. In the second approach based on an importance sampling technique, the expectation values of observables are evaluated stochastically by the importance sampling, instead of preparing the Gutzwiller wave function itself on a quantum computer. In general, this approach suffers from the sign problem (more precisely, the phase problem) as in the auxiliary-field quantum Monte Carlo method [64, 65].

A. Linear combination of unitary operators

As shown in Eq. (11), summing all the auxiliary fields $s_i = \pm 1$ for $i = 1, 2, \ldots, N_{\text{site}}$, the nonunitary Gutzwiller factor $e^{-g\hat{D}}$ is expressed as a linear combination of $2^{N_{\text{site}}}$ unitary operators, each of which is composed of a product of N_{site} unitary operators $e^{\pm 2i\alpha\hat{\eta}_i^z}$. Under the Jordan-Wigner transformation, the unitary operator $e^{\pm 2i\alpha\hat{\eta}_i^z}$ is then simply represented as a direct product of two single-qubit Z rotation gates acting on qubits $i_\uparrow$ and $i_\downarrow$, as shown in Eq. (21).

In order to implement the linear combination of these unitary operators on a quantum computer, we can use a Hadamard-test-like variant [66] of the quantum circuit known as the linear combination of unitary operators [67, 68], shown in Figs. 1(a) and 1(b) for $N_{\text{site}} = 1$ and 2, respectively, as examples, which can be easily generalized to $N_{\text{site}} \geqslant 3$. In these figures, we use N_{sites} ancillary qubits and measure each of them once. Instead, we can also consider the equivalent quantum circuit with only one ancillary qubit and every time after measuring it, we reuse this ancillary qubit repeatedly N_{site} times. This can certainly reduce the total number of necessary qubits, but has to initialize a qubit during the computation.

Figure 1(c) shows another way to simplify the quantum circuits in Figs. 1(a) and 1(b). Namely, the consecutive opposite-conditional controlled-$\hat{\eta}_i^z$-rotation gates with opposite rotation angles can be simplified by, for example, removing the "controlled" part from the first controlled-$\hat{\eta}_i^z$-rotation gate and doubling the rotation angle in the second controlled-$\hat{\eta}_i^z$-rotation gate. Such an operation can be implemented, under the Jordan-Wigner transformation, with 2 R_Z gates and 2 controlled-R_Z gates, instead of 4 controlled-R_Z gates, as shown in the lower part of Fig. 1(c). Following this strategy, the quantum circuit shown in Fig. 1(b) for $N_{\text{site}} = 2$ is now explicitly given in Fig. 1(d). We note that this simplification strategy is applicable not only for a quantum circuit containing two consecutive controlled-$\hat{\eta}_i^z$-rotation gates with opposite rotation angles but also for a quantum circuit containing two consecutive controlled-time-evolution operators with
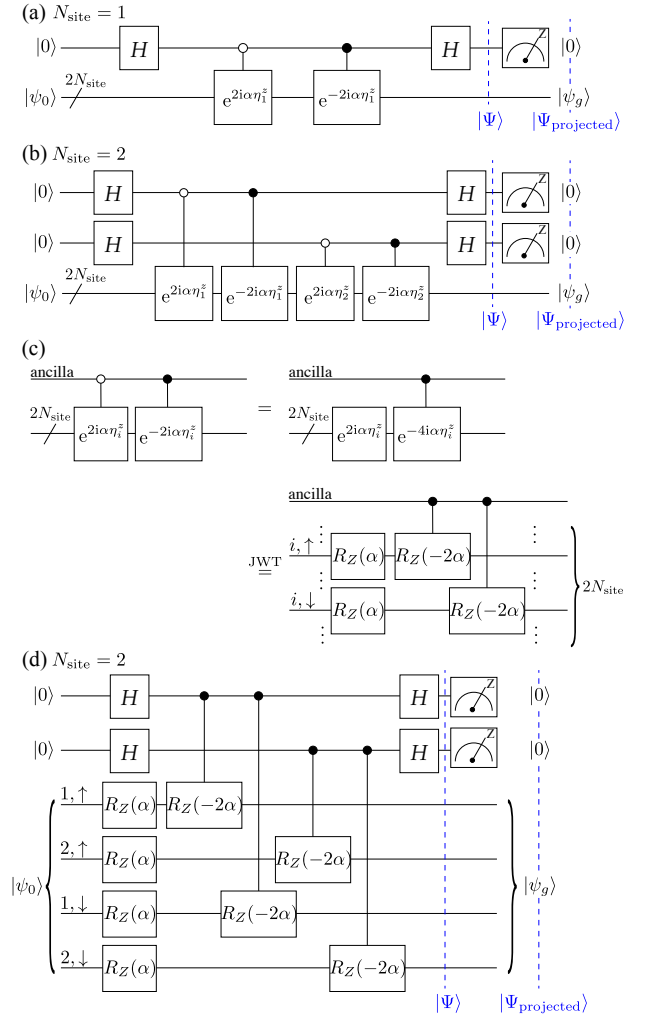

FIG. 1. Quantum circuits for generating the Gutzwiller wave function $|\psi_g\rangle$ with N_{site} ancillary qubits and $2N_{\text{site}}$ register qubits for (a) $N_{\text{site}} = 1$ and (b) $N_{\text{site}} = 2$. H denotes the Hadamard gate, $|\Psi\rangle$ denotes the state of the whole ($3N_{\text{site}}$-qubit) system after applying the second Hadamard gates on ancillary qubits, and $|\Psi_{\text{projected}}\rangle$ denotes the state of the whole system after observing that the state of the ancillary qubits is $|00\cdots0\rangle$. (c) Simplification of a product of the two consecutive controlled-$\hat{\eta}_i^z$-rotation gates with opposite rotation angles, assuming the Jordan-Wigner transformation in Eq. (21). (d) The same as (b) but the controlled-$\hat{\eta}_i^z$ gates are now explicitly written with the simplification strategy in (c).

opposite evolution times, and hence the quantum circuit proposed for the quantum power method in Ref. [66] (and also a recent proposal for performing the imaginary-time evolution in Ref. [58]) can be simplified in the same manner.

If the measured states in the N_{site} ancillary qubits are all found in the state $|0\rangle$, then the desirable state $\prod_{i=1}^{N_{\text{site}}} \sum_{s_i=\pm1} e^{2i\alpha s_i \hat{\eta}_i^z} |\psi_0\rangle$ is prepared in the rest of the qubits, i.e., in the $2N_{\text{site}}$ register qubits, as shown in Fig. 1(d). After applying the second Hadamard gates on the ancillary qubits,

the state $|\Psi\rangle$ of the whole system (see Fig. 1) is given as

$$|\Psi\rangle = |00\cdots0\rangle \otimes \frac{1}{2^{N_{\text{site}}}} \prod_{i=1}^{N_{\text{site}}} (e^{2i\alpha\hat{\eta}_i^z} + e^{-2i\alpha\hat{\eta}_i^z})|\psi_0\rangle$$

$$+ \text{(unwanted terms)}$$

$$= |00\cdots0\rangle \otimes e^{-gN_{\text{site}}/4}e^{-g\hat{D}}|\psi_0\rangle$$

$$+ \text{(unwanted terms)}. \tag{23}$$

Here, $|00\cdots0\rangle$ denotes the product state of all the N_{site} ancillary states being $|0\rangle$, and "(unwanted terms)" denotes the other $2^{N_{\text{sites}}} - 1$ terms with the N_{site} ancillary states being distinct from $|00\cdots0\rangle$, for which the Gutzwiller wave function $|\psi_g\rangle$ is not prepared in the register qubits. Note also that Eq. (11) is used in the second equality of Eq. (23). According to the Born rule, the probability for successfully preparing the desired state $|\psi_g\rangle$, denoted as $p_{00\cdots0}$, is given by

$$p_{00\cdots0} = \langle\Psi|\hat{\mathcal{P}}_{00\cdots0}|\Psi\rangle = e^{-gN_{\text{site}}/2}\langle\psi_0|e^{-2g\hat{D}}|\psi_0\rangle, \tag{24}$$

where $\hat{\mathcal{P}}_{00\cdots0} = |00\cdots0\rangle\langle00\cdots0|\otimes\hat{I}$ is the projection operator that projects a state in the whole Hilbert space onto the subspace associated with the result of the measurement observing that the state of the ancillary qubits is $|00\cdots0\rangle$. According to the projection postulate, the state after the corresponding (successful) measurement, denoted as $|\Psi_{\text{projected}}\rangle$, is then given by

$$|\Psi_{\text{projected}}\rangle = \frac{1}{\sqrt{p_{00\cdots0}}}\hat{\mathcal{P}}_{00\cdots0}|\Psi\rangle = |00\cdots0\rangle \otimes |\psi_g\rangle, \tag{25}$$

indicating that the Gutzwiller wave function $|\psi_g\rangle$ is prepared in the resister qubits.

Figure 2 shows the success probability $p_{00\cdots0}$ as functions of N_{site} and g calculated numerically using a classical computer. Here, the trial state $|\psi_0\rangle$ is chosen as the ground state of $\hat{K}$ at half filling defined on the one-dimensional chain under open-boundary conditions. As clearly observed in Fig. 2(a), the success probability $p_{00\cdots0}$ decrease exponentially in N_{site}. In order to examine the g dependence of $p_{00\cdots0}$, it is useful to study the logarithmic derivative of the success probability. It follows from Eq. (24) that the logarithmic derivative of the success probability, $\partial_g \ln p_{00\cdots0}$, is related to the expectation value of $\hat{D}$ via

$$\langle\psi_g|\hat{D}|\psi_g\rangle = -\frac{1}{2}\frac{\partial}{\partial g}\ln\langle\psi_0|e^{-2g\hat{D}}|\psi_0\rangle$$

$$= -\left(\frac{N_{\text{site}}}{4} + \frac{1}{2}\frac{\partial}{\partial g}\ln p_{00\cdots0}\right). \tag{26}$$

Since $\lim_{g\to0}\langle\psi_g|\hat{D}|\psi_g\rangle = 0$ and $\lim_{g\to\infty}\langle\psi_g|\hat{D}|\psi_g\rangle = -N_{\text{site}}/4$ for the present choice of $|\psi_0\rangle$, the slopes of $\ln p_{00\cdots0}$ in the two limits are given respectively by

$$\lim_{g\to0}\frac{\partial}{\partial g}\ln p_{00\cdots0} = -\frac{N_{\text{site}}}{2} \tag{27}$$

and

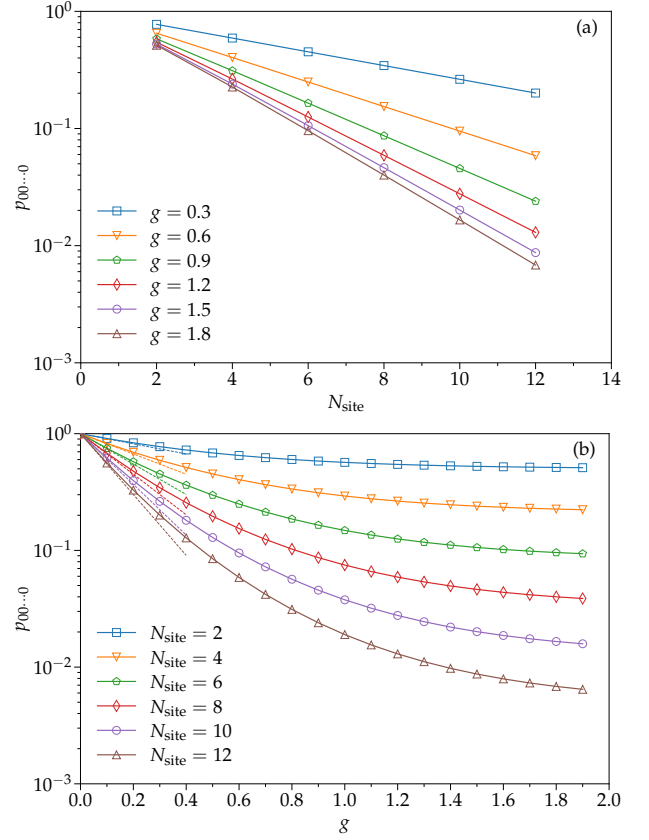$$\lim_{g\to\infty}\frac{\partial}{\partial g}\ln p_{00\cdots0} = 0, \tag{28}$$

FIG. 2. The success probability $p_{00\cdots0}$ (a) as a function of N_{site} for several values of g and (b) as a function of g for several values of N_{site}. The dashed lines in (b) indicate the exponential decrease of $p_{00\cdots0}$ for small g according to Eq. (27). The trial state $|\psi_0\rangle$ is chosen as the ground state of $\hat{K}$ at half filling defined on a one-dimensional chain under open-boundary conditions. Solid lines are guide for the eyes.

implying that $p_{00\cdots0}$ decreases exponentially in g for small g, but the decrease saturates for large g, as indeed found in Fig. 2(b). A finite success probability in the limit $g \to \infty$ leaves a possibility of preparing the Gutzwiller-projected state [69] relevant for the t-J-type models [70–76] for a moderate N_{site}.

Despite the exponential decrease of the success probability in N_{site}, an advantage of the approach described here is that the Gutzwiller wave function $|\psi_g\rangle$ itself can be prepared on a quantum computer. In this sense, the present scheme is similar to that in the previous study [53], even though the two schemes take different routes: the quantum circuit in Ref. [53] is based on the original form of the Gutzwiller factor in Eq. (5) with a slightly different parametrization, whereas the quantum circuit in the present study is based on the Hubbard-Stratonovich-transformed Gutzwiller factor in Eq. (11). It should be emphasized that the quantum circuit proposed here is rather simpler than that proposed in the previous study [53]. This point will be further discussed in Sec. V.

B. Importance sampling

1. Reformulation and sampling

To perform the sum $\sum_s$ over the auxiliary fields $s = \{\{s_{i,\tau}\}_{i=1}^{N_{\text{site}}}\}_{\tau=1}^2$ in Eq. (14) stochastically using the Monte Carlo method, we rewrite Eq. (14) as

$$\langle \hat{O} \rangle = \sum_s P_s \langle \hat{O} \rangle_s, \tag{29}$$

where

$$P_s \equiv \frac{\langle \psi_0 | \prod_{i=1}^{N_{\text{site}}} e^{2i\alpha(s_{i,1}+s_{i,2})\hat{\eta}_i^z} |\psi_0\rangle}{\sum_{s'} \langle \psi_0 | \prod_{i=1}^{N_{\text{site}}} e^{2i\alpha(s'_{i,1}+s'_{i,2})\hat{\eta}_i^z} |\psi_0\rangle} \tag{30}$$

and

$$\langle \hat{O} \rangle_s \equiv \frac{\langle \psi_0 | \prod_{i=1}^{N_{\text{site}}} e^{2i\alpha s_{i,2}\hat{\eta}_i^z} \hat{O} \prod_{j=1}^{N_{\text{site}}} e^{2i\alpha s_{j,1}\hat{\eta}_i^z} |\psi_0\rangle}{\langle \psi_0 | \prod_{i=1}^{N_{\text{site}}} e^{2i\alpha(s_{i,1}+s_{i,2})\hat{\eta}_i^z} |\psi_0\rangle}. \tag{31}$$

Notice that P_s is in general complex and hence the method suffers from the phase problem, as in the auxiliary-field Monte Carlo method [64, 65]. In the presence of the phase problem, a proper modification in Eq. (29) is necessary (see for example Refs. [77–79]). In this study, however, we only consider cases satisfying that P_s is real and $P_s > 0$, i.e., in the absence of the phase problem (see Appendix B).

The auxiliary fields in Eq. (29) are sampled by the Metropolis-Hastings algorithm using the local update with an acceptance probability $p(s \to s') = \min(1, P_{s'}/P_s)$ for accepting the move from s to s'. In the local update, the candidate auxiliary fields $s' = \{\{s'_{i,\tau}\}_{i=1}^{N_{\text{site}}}\}_{\tau=1}^2$ is chosen by flipping only a single auxiliary field, $s_{i,\tau} \to -s_{i,\tau}$, among the current auxiliary fields $s = \{\{s_{i,\tau}\}_{i=1}^{N_{\text{site}}}\}_{\tau=1}^2$ and the remaining auxiliary fields are unaltered. If the proposed move from s to s' is accepted, the candidate auxiliary fields s' are adopted as the new auxiliary fields for the next iteration. Otherwise, the old auxiliary fields s remain for the next iteration. Here, we select a flipped auxiliary field $s_{i,\tau}$ in the candidate auxiliary fields s' sequentially for $i = 1, 2, \ldots, N_{\text{site}}$ and $\tau = 1, 2$, and define one Monte Carlo sweep when all the auxiliary fields are selected once in the Monte Carlo iterations. We measure observables every Monte Carlo sweep and denote the number of measurements by N_{MC}. Note that we do not have to evaluate the denominator in Eq. (30) because only the ratio of $P_{s'}/P_s$ is required in the Monte Carlo iterations.

Using the relation in Eq. (21) for $\hat{\eta}_i$ under the Jordan-Wigner transformation, the numerator of P_s in Eq. (30) and the denominator of $\langle \hat{O} \rangle_s$ in Eq. (31) can be expressed with the Pauli operators as

$$\langle \psi_0 | \prod_{i=1}^{N_{\text{site}}} e^{2i\alpha(s_{i,1}+s_{i,2})\hat{\eta}_i^z} |\psi_0\rangle$$

$$\overset{\text{JWT}}{=} \langle \psi_0 | \prod_{i=1}^{N_{\text{site}}} \hat{R}_{Z_{i_\uparrow}}((s_{i,1}+s_{i,2})\alpha)\, \hat{R}_{Z_{i_\downarrow}}((s_{i,1}+s_{i,2})\alpha) |\psi_0\rangle, \tag{32}$$
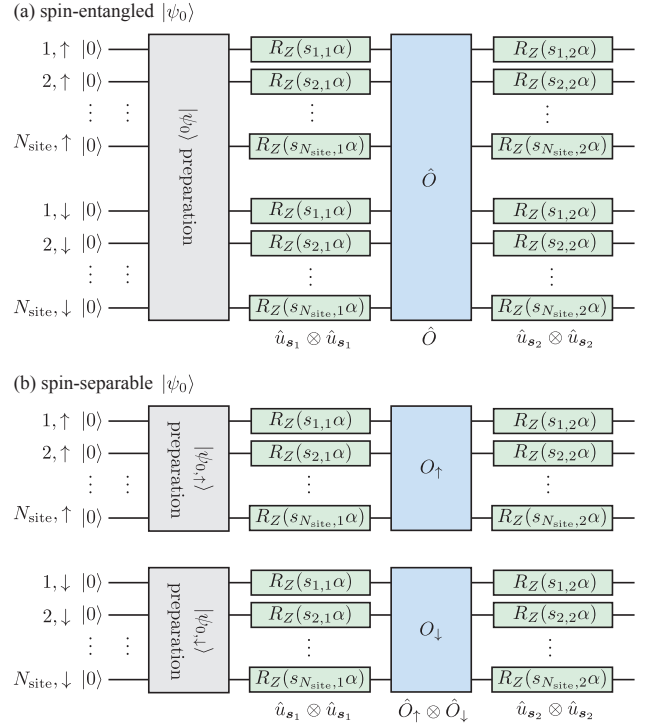

FIG. 3. Quantum circuits for preparing the state $\prod_i e^{2i\alpha s_{i,2}\hat{\eta}_i^z} \hat{O} \prod_i e^{2i\alpha s_{i,1}\hat{\eta}_i^z} |\psi_0\rangle$ appearing in the numerator of Eq. (31) for (a) a spin-entangled state $|\psi_0\rangle$ and (b) a spin-separable state $|\psi_0\rangle$, assuming the Jordan-Wigner transformation. We also assume that the observable $\hat{O}$ is spin-separable in (b).

where the symbol "$\otimes$" for a direct product is omitted for simplicity. Similarly, the numerator of $\langle \hat{O} \rangle_s$ in Eq. (31) can be given as

$$\langle \psi_0 | \prod_{i=1}^{N_{\text{site}}} e^{2i\alpha s_{i,2}\hat{\eta}_i^z} \hat{O} \prod_{j=1}^{N_{\text{site}}} e^{2i\alpha s_{j,1}\hat{\eta}_i^z} |\psi_0\rangle$$

$$\overset{\text{JWT}}{=} \langle \psi_0 | \prod_{i=1}^{N_{\text{site}}} \hat{R}_{Z_{i_\uparrow}}(s_{i,2}\alpha)\hat{R}_{Z_{i_\downarrow}}(s_{i,2}\alpha) \hat{O} \prod_{j=1}^{N_{\text{site}}} \hat{R}_{Z_{j_\uparrow}}(s_{j,1}\alpha)\hat{R}_{Z_{j_\downarrow}}(s_{j,1}\alpha) |\psi_0\rangle. \tag{33}$$

Therefore, as shown in Fig. 3(a), a quantum circuit for preparing the state $\prod_i e^{2i\alpha s_{i,2}\hat{\eta}_i^z} \hat{O} \prod_i e^{2i\alpha s_{i,1}\hat{\eta}_i^z} |\psi_0\rangle$ in the numerator of $\langle \hat{O} \rangle_s$ in Eq. (31) is significantly simple. A quantum circuit for the state $\prod_{i=1}^{N_{\text{site}}} e^{2i\alpha(s_{i,1}+s_{i,2})\hat{\eta}_i^z} |\psi_0\rangle$ in the denominator of $\langle \hat{O} \rangle_s$ in Eq. (31) can be obtained by simply setting $\hat{O} = \hat{I}$ and combining the two rotation gates $\hat{R}_{Z_{i_\sigma}}(s_{i,1}\alpha)$ and $\hat{R}_{Z_{i_\sigma}}(s_{i,2}\alpha)$ into the single rotation $\hat{R}_{Z_{i_\sigma}}((s_{i,1}+s_{i,2})\alpha)$ in Fig. 3(a).

2. Simplification for spin-separable states

Next, we describe a simplification that can be applied when the trial state $|\psi_0\rangle$ is separable according to the decomposition of the Hilbert space $\mathcal{V} = \mathcal{V}_\uparrow \otimes \mathcal{V}_\downarrow$, where $\mathcal{V}_\sigma$ denotes the

Hilbert space for fermions with spin σ. Let us assume that $|\psi_0\rangle$ is a separable state of the form

$$|\psi_0\rangle = |\psi_{0,\uparrow}\rangle \otimes |\psi_{0,\downarrow}\rangle, \qquad (34)$$

where $|\psi_{0,\sigma}\rangle \in \mathcal{V}_\sigma$, as in the case for the ground state of $\hat{K}$. We refer to a state of the form in Eq. (34) as a spin-separable state.

Let us now introduce the following unitary operator

$$\hat{u}_{s_\tau,\sigma} \equiv \prod_{i=1}^{N_{\text{site}}} e^{i\alpha s_{i,\tau}(\hat{n}_{i\sigma} - \frac{1}{2})} \overset{\text{JWT}}{=} \prod_{i=1}^{N_{\text{site}}} \hat{R}_{Z_{i\sigma}}(s_{i,\tau}\alpha) \qquad (35)$$

on $\mathcal{V}_\sigma$ for a given set of auxiliary fields $s_{i,\tau} = \{s_{i,\tau}\}_{i=1}^{N_{\text{site}}}$. The last equality is simply because $\hat{n}_{i\sigma} \overset{\text{JWT}}{=} \frac{1}{2}(1 - \hat{Z}_{i\sigma})$ under the Jordan-Wigner transformation. Then the product of unitary operators generated by $\hat{\eta}_i^z$ can be written as

$$\prod_{i=1}^{N_{\text{site}}} e^{2i\alpha(s_{i,1} + s_{i,2})\hat{\eta}_i} = \hat{u}_{s_2,\uparrow} \hat{u}_{s_1,\uparrow} \otimes \hat{u}_{s_2,\downarrow} \hat{u}_{s_1,\downarrow}. \qquad (36)$$

Therefore, P_s and $\langle \hat{O} \rangle_s$ in Eqs. (30) and (31) are given respectively as

$$P_s = \frac{\langle \psi_{0,\uparrow}|\hat{u}_{s_2,\uparrow}\hat{u}_{s_1,\uparrow}|\psi_{0,\uparrow}\rangle \langle \psi_{0,\downarrow}|\hat{u}_{s_2,\downarrow}\hat{u}_{s_1,\downarrow}|\psi_{0,\downarrow}\rangle}{\sum_{s'} \langle \psi_{0,\uparrow}|\hat{u}_{s_2',\uparrow}\hat{u}_{s_1',\uparrow}|\psi_{0,\uparrow}\rangle \langle \psi_{0,\downarrow}|\hat{u}_{s_2',\downarrow}\hat{u}_{s_1',\downarrow}|\psi_{0,\downarrow}\rangle} \qquad (37)$$

and

$$\langle \hat{O} \rangle_s = \frac{\langle \psi_{0,\uparrow}|\hat{u}_{s_2,\uparrow}\hat{O}_\uparrow \hat{u}_{s_1,\uparrow}|\psi_{0,\uparrow}\rangle}{\langle \psi_{0,\uparrow}|\hat{u}_{s_2,\uparrow}\hat{u}_{s_1,\uparrow}|\psi_{0,\uparrow}\rangle} \cdot \frac{\langle \psi_{0,\downarrow}|\hat{u}_{s_2,\downarrow}\hat{O}_\downarrow \hat{u}_{s_1,\downarrow}|\psi_{0,\downarrow}\rangle}{\langle \psi_{0,\downarrow}|\hat{u}_{s_2,\downarrow}\hat{u}_{s_1,\downarrow}|\psi_{0,\downarrow}\rangle}, \qquad (38)$$

where the observable of the form

$$\hat{O} = \hat{O}_\uparrow \otimes \hat{O}_\downarrow \qquad (39)$$

is assumed. A quantum circuit for preparing the state $\prod_i e^{2i\alpha s_{i,2}\hat{\eta}_i^z} \hat{O} \prod_i e^{2i\alpha s_{i,1}\hat{\eta}_i^z} |\psi_0\rangle$ in the numerator of $\langle \hat{O} \rangle_s$ in Eq. (31) is now further simplified as shown in Fig. 3(b). A quantum circuit for the state $\prod_{i=1}^{N_{\text{site}}} e^{2i\alpha(s_{i,1}+s_{i,2})\hat{\eta}_i^z} |\psi_0\rangle$ in the denominator of $\langle \hat{O} \rangle_s$ in Eq. (31) can be obtained by simply setting $\hat{O} = \hat{I}$ and combining two consecutive rotations into one in Fig. 3(b). Notice that when $|\psi_0\rangle$ is a spin-separable state, only N_{site} qubits are required at a time.

Finally, we note that since the kinetic term of the Hamiltonian has the form,

$$\hat{K} = \hat{K}_\uparrow \otimes \hat{I} + \hat{I} \otimes \hat{K}_\downarrow, \qquad (40)$$

where $\hat{K}_\sigma$ is the summand of $\sum_\sigma$ in Eq. (2), $\langle \hat{K} \rangle_s$ can be written simply as

$$\langle \hat{K} \rangle_s = \frac{\langle \psi_{0,\uparrow}|\hat{u}_{s_2}\hat{K}_\uparrow \hat{u}_{s_1}|\psi_{0,\uparrow}\rangle}{\langle \psi_{0,\uparrow}|\hat{u}_{s_2}\hat{u}_{s_1}|\psi_{0,\uparrow}\rangle} + \frac{\langle \psi_{0,\downarrow}|\hat{u}_{s_2}\hat{K}_\downarrow \hat{u}_{s_1}|\psi_{0,\downarrow}\rangle}{\langle \psi_{0,\downarrow}|\hat{u}_{s_2}\hat{u}_{s_1}|\psi_{0,\downarrow}\rangle}. \qquad (41)$$

A similar formula is also obtained for $\langle \hat{D} \rangle_s$.

3. Numerical simulations

To demonstrate the method proposed here, we employ a classical computer to evaluate numerical the expectation values of the total energy $E = \langle \hat{K} \rangle + U\langle \hat{D} \rangle$, the kinetic energy $\langle \hat{K} \rangle$, and the potential energy $U\langle \hat{D} \rangle$ as a function of g for several U values. The trial state $|\psi_0\rangle$ is chosen as the ground state of $\hat{K}$, which is a spin-separable state, and in this case the Monte Carlo importance sampling can be performed without the phase problem. Although we use a classical computer to demonstrate the method proposed here, we briefly comment on how to prepare the trial state $|\psi_0\rangle$ on a quantum computer. Generally, a Slater-determinant state can be prepared on a quantum computer with at most $O(N_{\text{site}}^2)$ number of two-qubit (e.g., Givens) rotation gates starting from a relevant product state [80–82]. A concrete example of variationally preparing the ground state of $\hat{K}$ in one dimension using a discretized quantum-adiabatic process can be found in Ref. [83].

Figure 4 shows the results for Fermi-Hubbard model in three different lattices with $N_{\text{MC}} = 20000$ and $N_{\text{MC}} = 80000$. For comparison, the exact results as well as the results obtained by fully summing all the auxiliary fields are also shown. Although the proposed method can reproduce the exact results within the statistical errors, we find that the total energy E has the larger statistical errors for larger U/J in all the three lattices. By resolving the total energy E into the kinetic and the potential energies, we find that the kinetic energy has the much smaller statistical errors than the potential energy. Therefore, the large statistical errors in E are mainly due to the large statistical errors in the potential energy, i.e., the expectation value of $\hat{D}$. We note that the larger statistical errors in the potential energy are due to the choice of the auxiliary fields, which are coupled to the local fermion-density operator $\hat{\eta}_i^z$: if the auxiliary fields are coupled to the local spin operator [59] (although in this case the Gutzwiller factor is no longer expressed as a linear combination of unitary operators and hence this is less relevant in the context of this study), the fluctuation of $\langle \hat{D} \rangle$ can be suppressed.

IV. DEMONSTRATION ON A QUANTUM DEVICE

In this section, we shall use a NISQ device to demonstrate the proposed method for the two-site Fermi-Hubbard model. As described below, the Gutzwiller wave function can describe the exact ground state of the two-site Fermi-Hubbard model.

A. Gutzwiller wave function for the two-site Fermi-Hubbard model at half filling

First, we review the well-known fact that the ground state of the two-site Fermi-Hubbard model at half filling can be described by the Gutzwiller wave function with $|\psi_0\rangle$ being the ground state of $\hat{K}$ (for example, see Ref. [41]). Let $|\text{vac}\rangle$ be the fermion vacuum such that $\hat{c}_{i\sigma}|\text{vac}\rangle = 0$ for any site i and spin σ. Then the ground state of $\hat{K}$ at half filling is given by
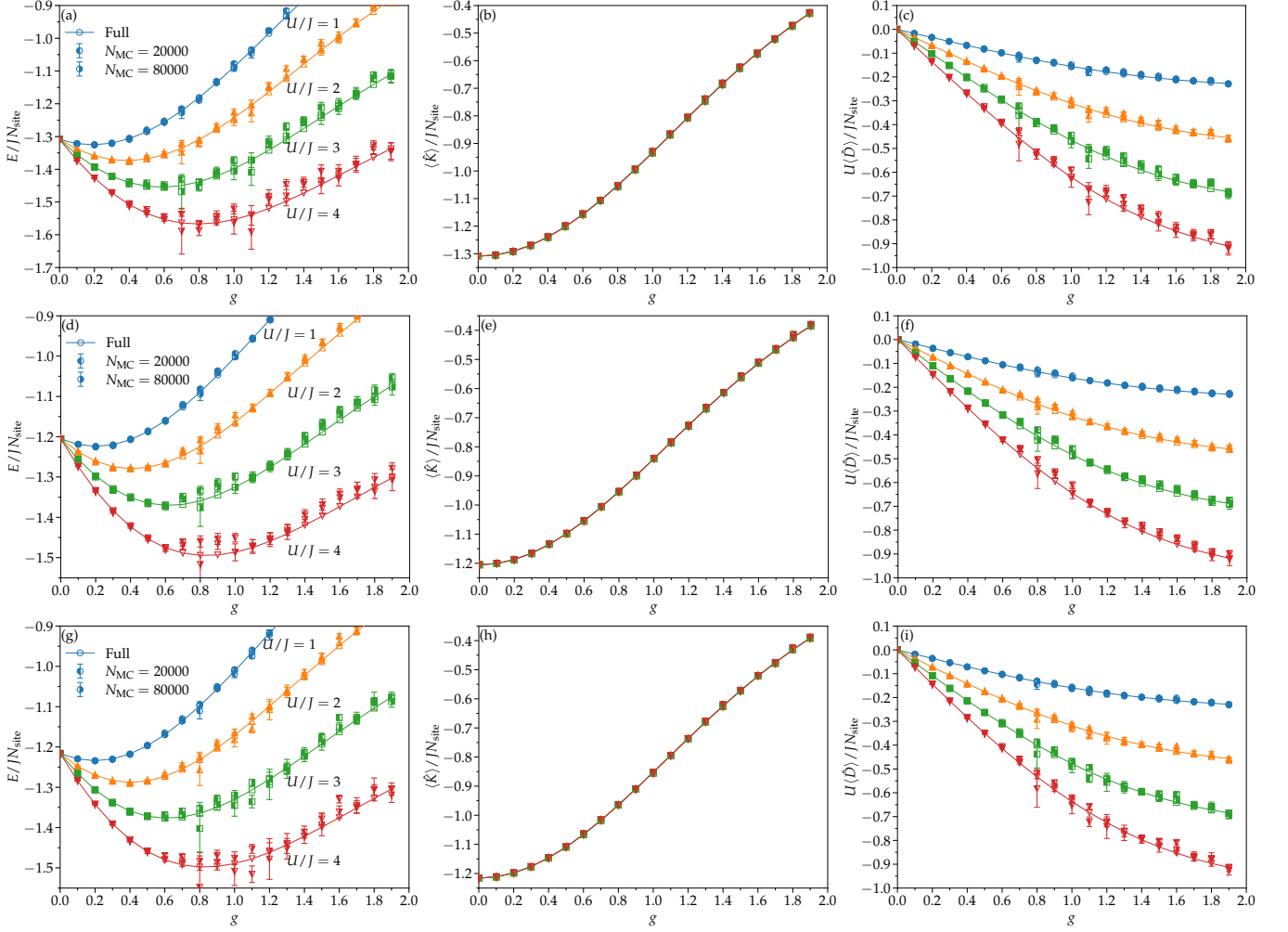
FIG. 4. The expectation values of (a, d, g) the total energy E, (b, e, h) the kinetic energy $\langle\hat{K}\rangle$, and (c, f, i) the potential energy $U\langle\hat{D}\rangle$ as a function of the Gutzwiller parameter g for the Fermi-Hubbard model at half filling with $U/J = 1, 2, 3, 4$ (top to bottom). The models studied here are on (a-c) a 4×2 ladder lattice, (d-f) a 10-site one-dimensional lattice, and (g-i) a 12-site one-dimensional lattice under open-boundary conditions. The number N_{MC} of Monte Carlo samplings is indicated in the figure. For comparison, the exact results are also plotted by solid lines. In addition, the results obtained by fully summing all the auxiliary fields are shown by open symbols. Note that $\langle\hat{K}\rangle$ does not depends on the value of U. The results of $\langle\hat{K}\rangle$ for two different N_{MC} values and obtained by fully summing all the auxiliary fields are indistinguishable in this scale.

the following state with two fermions occupying the bonding orbital:

$$|\psi_0\rangle = \frac{1}{2}\left(\hat{c}_{1\uparrow}^{\dagger} + \hat{c}_{2\uparrow}^{\dagger}\right)\left(\hat{c}_{1\downarrow}^{\dagger} + \hat{c}_{2\downarrow}^{\dagger}\right)|\mathrm{vac}\rangle. \tag{42}$$

A straightforward calculation shows that $\langle\psi_0|\mathrm{e}^{-g\hat{D}}\hat{K}\mathrm{e}^{-g\hat{D}}|\psi_0\rangle = -2J$, $\langle\psi_0|\mathrm{e}^{-2g\hat{D}}|\psi_0\rangle = \cosh g$, and $\langle\psi_0|\mathrm{e}^{-g\hat{D}}\hat{D}\mathrm{e}^{-g\hat{D}}|\psi_0\rangle = -\frac{1}{2}\partial_g\langle\psi_0|\mathrm{e}^{-2g\hat{D}}|\psi_0\rangle = -\frac{1}{2}\sinh g$. Therefore, the total energy $E(g)$ is given by

$$E(g) = \langle\hat{K}\rangle + U\langle\hat{D}\rangle$$
$$= -\frac{1}{\cosh g}\left(2J + \frac{U}{2}\sinh g\right). \tag{43}$$

Considering $E(g)$ as the variational energy, the stationary condition $\partial E(g)/\partial g|_{g=g_{\mathrm{opt}}} = 0$ gives us the optimal variational

parameter g_{opt} such that

$$\sinh g_{\mathrm{opt}} = \frac{U}{4J}, \tag{44}$$

or equivalently $g_{\mathrm{opt}} = \ln\left(\frac{U}{4J} + \sqrt{\left(\frac{U}{4J}\right)^2 + 1}\right)$. By substituting Eq. (44) into Eq. (43), the optimized variational energy is obtained as

$$E(g_{\mathrm{opt}}) = -\sqrt{4J^2 + \frac{U^2}{4}}, \tag{45}$$

which coincides with the exact ground-state energy of the two-site Fermi-Hubbard model at half filling, implying that the Gutzwiller wave function $|\psi_g\rangle$ with $g = g_{\mathrm{opt}}$ is the exact

ground state of the two-site Fermi-Hubbard model at half filling.

B. Quantum simulations

Using a real quantum device, we shall now evaluate the expectation values of the total energy E, the kinetic energy $\langle \hat{K} \rangle$, and the potential energy $U\langle \hat{D} \rangle$ with respect to the Gutzwiller wave function $|\psi_g\rangle$ for the two-site Fermi-Hubbard model at half filling. Under the Jordan-Wigner transformation, the fermion vacuum is expressed as $|\text{vac}\rangle \overset{\text{JWT}}{=} |0\rangle_{1_\uparrow}|0\rangle_{2_\uparrow}|0\rangle_{1_\downarrow}|0\rangle_{2_\downarrow}$ and hence $|\psi_0\rangle$ in Eq. (42), i.e., the ground state of $\hat{K}$, is given by $|\psi_0\rangle = |\psi_{0,\uparrow}\rangle \otimes |\psi_{0,\downarrow}\rangle$ with

$$|\psi_{0,\sigma}\rangle = \frac{1}{\sqrt{2}}\left(|0\rangle_{1_\sigma}|1\rangle_{2_\sigma} + |1\rangle_{1_\sigma}|0\rangle_{2_\sigma}\right). \quad (46)$$

This state $|\psi_{0,\sigma}\rangle$ is merely one of the Bell states and is easily prepared as

$$|\psi_{0,\sigma}\rangle = \widehat{CX}\left(\hat{H} \otimes \hat{X}\right)|0\rangle_{1_\sigma}|0\rangle_{2_\sigma}, \quad (47)$$

where $\hat{X}$, $\hat{H}$ and $\widehat{CX}$ denote the gate operations for Pauli X, Hadamard, and controlled-X (CNOT) gates, respectively. As discussed in Sec. III B 2, for the spin-separable trial state $|\psi_0\rangle$, the numerator of Eq. (14) is expressed as

$$\langle\psi_0|e^{-g\hat{D}}\hat{O}_\uparrow \otimes \hat{O}_\downarrow e^{-g\hat{D}}|\psi_0\rangle = \gamma^4 \sum_s \prod_{\sigma=\uparrow,\downarrow} P_{s\sigma}^{O_1 O_2}(g) \quad (48)$$

with

$$P_{s\sigma}^{O_1 O_2}(g) \equiv \langle\psi_{0,\sigma}|\hat{u}_{s_2,\sigma}\hat{O}_{1_\sigma}\hat{O}_{2_\sigma}\hat{u}_{s_1,\sigma}|\psi_{0,\sigma}\rangle, \quad (49)$$

where $\hat{O}_\sigma = \hat{O}_{1_\sigma}\hat{O}_{2_\sigma}$ and $\hat{O}_{i_\sigma} = \{\hat{I}_{i_\sigma}, \hat{X}_{i_\sigma}, \hat{Y}_{i_\sigma}, \hat{Z}_{i_\sigma}\}$. Here, $\hat{I}_{i_\sigma}$ is the identity operator acting on the i_σ qubit. Noticing that $\hat{u}_{s_1,\sigma} \neq \hat{u}_{s_2,\sigma}$ in general, we can not use the direct measurement method to evaluate the expectation value of Eq. (49), at least in a simple way [84]. Alternatively, we exploit the Hadamard test to measure the expectation value of the unitary operator $\hat{u}_{s_2,\sigma}\hat{O}_\sigma\hat{u}_{s_1,\sigma}$ [85]. The specific form of the Hamiltonian for the two-site Fermi-Hubbard model is simply given by $\hat{\mathcal{H}} = \hat{K} + U\hat{D}$ with $\hat{K} \overset{\text{JWT}}{=} -\frac{J}{2}\sum_{\sigma=\uparrow,\downarrow}\left(\hat{X}_{1_\sigma}\hat{X}_{2_\sigma} + \hat{Y}_{1_\sigma}\hat{Y}_{2_\sigma}\right)$ and $\hat{D} \overset{\text{JWT}}{=} \frac{1}{4}\sum_{i=1,2}\hat{Z}_{i_\uparrow}\hat{Z}_{i_\downarrow}$. Therefore, it is sufficient to evaluate $P_{s\uparrow}^{II}(g)$, $P_{s\uparrow}^{ZI}(g)$, and $P_{s\uparrow}^{XX}(g)$ to calculate $\langle\hat{K}\rangle$ and $\langle\hat{D}\rangle$, and thereby the total energy E. Instead of employing the importance sampling, here we directly perform the sum over all the auxiliary fields, $\sum_s \cdots = \sum_{s_{1,1}=\pm1}\sum_{s_{2,1}=\pm1}\sum_{s_{1,2}=\pm1}\sum_{s_{2,2}=\pm1}\cdots$, because the total number of terms is only $2^4 = 16$.

Figure 5 shows the quantum circuits for estimating the expectation values $P_{s\uparrow}^{II}(g)$, $P_{s\uparrow}^{ZI}(g)$, and $P_{s\uparrow}^{XX}(g)$. Notice that here we explicitly introduce the SWAP operations in order to involve only two-qubit gates acting on neighboring qubits in these quantum circuits. To further simplify the quantum circuits, the second SWAP gate that would have primarily been placed after the last Z rotation in each quantum circuit is omitted without affecting validity of the measurement. This latter simplification, yielding reduction of three CNOT gates, is beneficial for suppressing noise inherent to a real quantum device.

We implement the quantum circuits using the Quantum Information Software Kit (Qiskit) [86] and perform computations on the IBM Q Manila device (`ibmq_manila`), the device publicly available through the IBM Quantum Lab platform [87]. We also run the same quantum circuits on the classical simulator (`qasm_simulator`), which is considered as an ideal quantum device, to realize the impact of noise. Each experiment runs 8192 shots to measure the local state at the ancillary qubit in the computational basis. The same set of experiments is repeated 16 times to evaluate the average and the standard deviation, the latter being the estimate of the statistical error.

Figure 6 shows the results for the denominator of Eq. (14) and the numerators for $\langle\hat{Z}_{1_\uparrow}\hat{Z}_{1_\downarrow}\rangle$ and $\langle\hat{X}_{1_\uparrow}\hat{X}_{2_\uparrow}\rangle$, which are calculated respectively as

$$\langle\psi_0|e^{-2g\hat{D}}|\psi_0\rangle = \left(\sum_s P_{s\uparrow}^{II}(g)\right)^2, \quad (50)$$

$$\langle\psi_0|e^{-g\hat{D}}\hat{Z}_{1_\uparrow}\hat{Z}_{1_\downarrow}e^{-g\hat{D}}|\psi_0\rangle = \left(\sum_s P_{s\uparrow}^{ZI}(g)\right)^2, \quad (51)$$

and

$$\langle\psi_0|e^{-g\hat{D}}\hat{X}_{1_\uparrow}\hat{X}_{2_\uparrow}e^{-g\hat{D}}|\psi_0\rangle = \left(\sum_s P_{s\uparrow}^{XX}(g)\right)\left(\sum_s P_{s\uparrow}^{II}(g)\right). \quad (52)$$

Here, we utilize the equivalence between fermion spins $\uparrow$ and $\downarrow$. Despite the simple quantum circuits, we notice the sizable discrepancies between the results computed directly from the real quantum device and the analytical results. The discrepancies are more noticeable for $\langle\psi_0|e^{-g\hat{D}}\hat{X}_{1_\uparrow}\hat{X}_{2_\uparrow}e^{-g\hat{D}}|\psi_0\rangle$, as shown in Fig. 6(c), since the evaluation of $P_{s\uparrow}^{XX}(g)$ involves more CNOT gates than the others (see Fig. 5).

To mitigate the systematic errors, we apply a so-called phase-and-scale (PaS) correction technique developed in the study of spin dynamics [88, 89]. Since the ideal value of $P_{s\uparrow}^{II}(g)$ at $g = 0$ is know to be one for all s, in the PaS correction method, the inverse of the raw data of $P_{s\uparrow}^{II}(0)$ is multiplied to the raw data of $P_{s\uparrow}^{II}(g)$ to mitigate the systematic errors. The same strategy is applied to $P_{s\uparrow}^{XX}(g)$ because $|\psi_0\rangle$ is chosen as the ground state of $\hat{K}$, i.e., a spin singlet state. On the other hand, for the error mitigation in $P_{s\uparrow}^{ZI}(g)$, we use the raw data at a sufficiently large g, i.e., $g = 10$, so as to reproduce the value in the strong coupling limit, where the rotation angle α is simply $\frac{\pi}{2}$. This simple technique is found to successfully mitigate the most of the systematic errors, as shown in Fig. 6. Finally, the total energy E as well as the kinetic energy $\langle\hat{K}\rangle$ and the potential energy $U\langle\hat{D}\rangle$ calculated from these error-mitigated values is shown in Fig. 7. We find that these results are in good agreement with the analytical results within the error bars. We note that the PaS correction technique can in principle be applied for larger systems because the exact values of $\langle\hat{K}\rangle$ with $g = 0$ in the noninteracting limit and $\langle\hat{D}\rangle$ with $g \gg 1$ in the atomic limit can be evaluated efficiently with classical computers or even analytically.
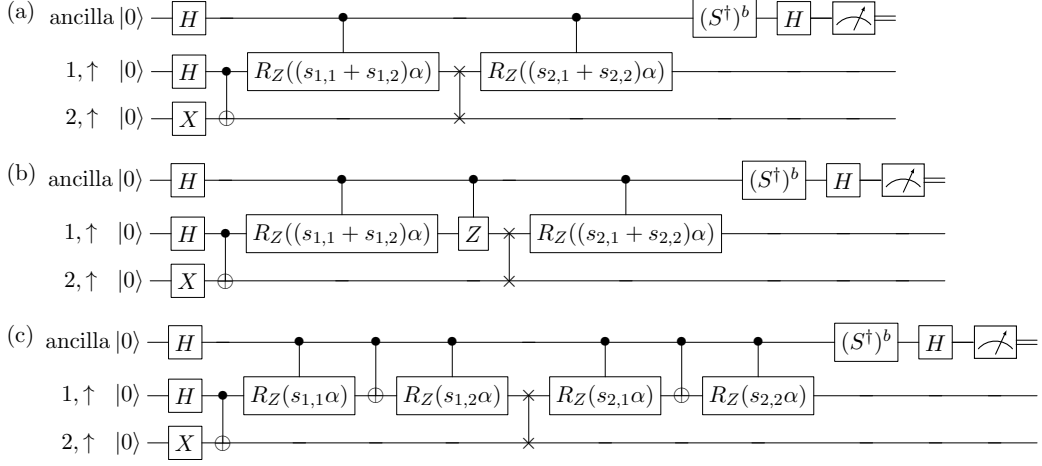
FIG. 5. Quantum circuits for the Hadamard test to evaluate the expectation values of (a) $P_{s\uparrow}^{II}(g) = \langle\psi_{0\uparrow}|\hat{u}_{s_2,\uparrow}\hat{u}_{s_1,\uparrow}|\psi_{0\uparrow}\rangle$, (b) $P_{s\uparrow}^{ZI}(g) = \langle\psi_{0\uparrow}|\hat{u}_{s_2,\uparrow}\hat{Z}_{1\uparrow}\hat{u}_{s_1,\uparrow}|\psi_{0\uparrow}\rangle$, and (c) $P_{s\uparrow}^{XX}(g) = \langle\psi_{0\uparrow}|\hat{u}_{s_2,\uparrow}\hat{X}_{1\uparrow}\hat{X}_{2\uparrow}\hat{u}_{s_1,\uparrow}|\psi_{0\uparrow}\rangle$. The real and imaginary part of each expectation value are estimated as $P_0 - P_1$ for $b = 0$ and 1, respectively. Here, P_0 is the probability of measuring $|0\rangle$ at the ancillary qubit and $P_1 = 1 - P_0$. The SWAP gate is denoted by a line connecting two crosses. $S^\dagger$ denotes the single-qubit phase shift gate acting as $\hat{S}^\dagger|0\rangle_{i_\sigma} = |0\rangle_{i_\sigma}$ and $\hat{S}^\dagger|1\rangle_{i_\sigma} = -i|1\rangle_{i_\sigma}$.
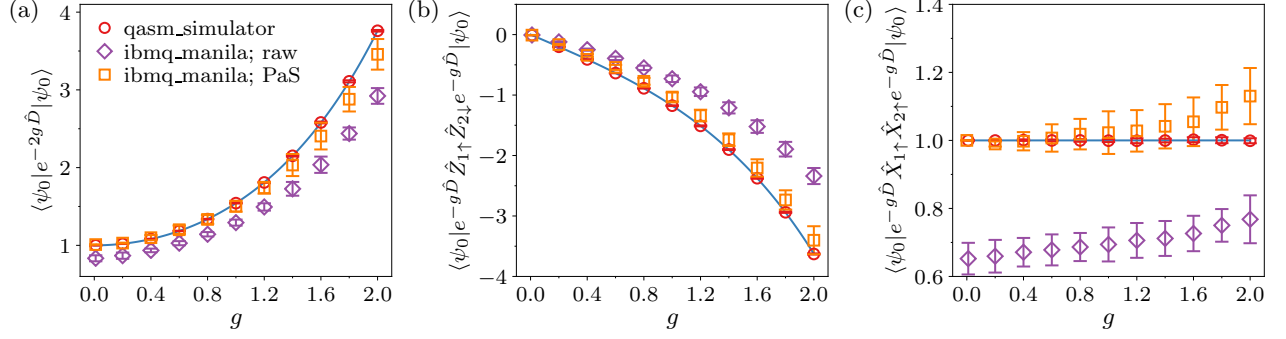

FIG. 6. Results of (a) $\langle\psi_0|e^{-2g\hat{D}}|\psi_0\rangle$, (b) $\langle\psi_0|e^{-g\hat{D}}\hat{Z}_{1\uparrow}\hat{Z}_{1\downarrow}e^{-g\hat{D}}|\psi_0\rangle$, and (c) $\langle\psi_0|e^{-g\hat{D}}\hat{X}_{1\uparrow}\hat{X}_{2\uparrow}e^{-g\hat{D}}|\psi_0\rangle$ as a function of the Gutzwiller parameter g. The results evaluated from the raw data obtained from the IBM Q Manila device are denoted by diamonds, and those after the error mitigation by the PaS correction technique are shown by squares. For comparison, the results calculated on the classical simulator (`qasm_simulator`) using the same quantum circuits are also plotted by circles, which agree with the analytical results shown by solid lines.

V. CONCLUSION AND DISCUSSION

Based on the discrete Hubbard-Stratonovich transformation of the Gutzwiller factor $e^{-g\hat{D}}$, we have proposed a scheme to implement the Gutzwiller wave function on a quantum computer and demonstrated it using numerical simulations and a real quantum device. The crucial point is that the nonunitary Gutzwiller factor $e^{-g\hat{D}}$ is expressed as a linear combination of unitary operators by introducing the auxiliary fields of the discrete Hubbard-Stratonovich transformation. The sum over the auxiliary fields generates an exponentially large number of terms with respect to the system size N_{site}, which is here treated by two complementary approaches, one employing a quantum circuit of the linear combination of unitaries to probabilistically prepare the Gutzwiller wave function on a quantum computer and the other using the importance sampling to stochastically evaluate the expectation values for the Gutzwiller wave function.

The first approach performs the sum over all the auxiliary fields by measuring the state of the N_{site} ancillary qubits. Although the success probability decreases exponentially in N_{site}, an advantage of this approach is that the Gutzwiller wave function $|\psi_g\rangle$ itself can be prepared on a quantum computer. In this sense, this approach is similar to that reported in Ref. [53]. Indeed, using Eqs. (5) and (7), one can show that the success probability $p_{00\cdots0}$ is exactly the same as that in Ref. [53]. Interestingly, however, the circuit structure is different from that in Ref. [53], as summarized in Table I. While N_{site} controlled-controlled-R_Y (CCR_Y) gates are required for preparing the Gutzwiller wave function in the previous study [53], assuming the Jordan-Wigner transformation, here $2N_{\text{site}}$ CR_Z gates are used for the same purpose. In terms of the number of CNOT gates, the implementation of a CR_Z gate is simpler than that of a CCR_Y gate because a CR_Z gate can be decomposed into 2 CNOT gates and 2 R_Z gates, while a CCR_Y gate can be decomposed into 2 Toffoli gates and 2 R_Y gates [90]. The CNOT gate
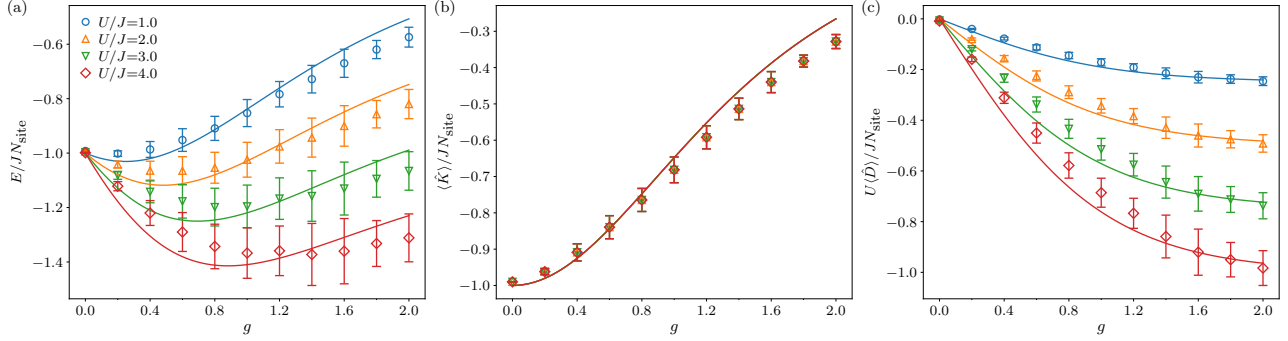
FIG. 7. The expectation values of (a) the total energy E, (b) the kinetic energy $\langle \hat{K} \rangle$, and (c) the potential energy $U\langle \hat{D} \rangle$ as a function of the Gutzwiller parameter g for the two-site ($N_{\text{site}} = 2$) Fermi-Hubbard model under open-boundary conditions at half filling with $U/J = 1, 2, 3, 4$ (top to bottom). The results are obtained from the error-mitigated values shown in Fig. 6. For comparison, the exact analytical results are also plotted by solid lines.

counts for decomposing 2 CR_Z gates is thus 4, whereas that for decomposing a single CCR_Y gate is 12 because a Toffoli gate requires 6 CNOT gates [91]. Therefore, in terms of the CNOT gate counts, the present scheme is beneficial for preparing the Gutzwiller wave function on a quantum computer.

We should emphasize that this simplification of the quantum circuit is made possible because our quantum circuit is inspired by the Hubbard-Stratonovich transformation. The Hubbard-Stratonovich transformation allows us to disentangle the two-body operator $e^{-g(\hat{n}_{i\uparrow} - \frac{1}{2})(\hat{n}_{i\downarrow} - \frac{1}{2})}$ into a linear combination of one-body operators $\propto e^{i\alpha(\hat{n}_{i\uparrow} + \hat{n}_{i\downarrow} - 1)} + e^{-i\alpha(\hat{n}_{i\uparrow} + \hat{n}_{i\downarrow} - 1)}$, each of which is then represented simply as a direct product of single-qubit rotations $R_{Z_{i\uparrow}} \otimes R_{Z_{i\downarrow}}$ under the Jordan-Wigner transformation.

Note, however, that the quantum circuit for taking the linear combination of the one-body operators $\frac{1}{2}(e^{i\alpha(\hat{n}_{i\uparrow} + \hat{n}_{i\downarrow} - 1)} + e^{-i\alpha(\hat{n}_{i\uparrow} + \hat{n}_{i\downarrow} - 1)})$ shown in Fig. 1 can also be expressed with controlled-controlled-unitary gates, as shown in Fig. 8. In Fig. 8, $\mathbf{0}$ is the 2×2 null matrix, $\mathbf{I}$ is the 2×2 identity matrix, and the Hadamard, Z-rotation, and X-rotation matrices are given by

$$\mathbf{H} = \frac{1}{\sqrt{2}}\begin{bmatrix} 1 & 1 \\ 1 & -1 \end{bmatrix}, \tag{53}$$

$$\mathbf{R}_Z(\alpha) = \begin{bmatrix} e^{-i\alpha/2} & 0 \\ 0 & e^{i\alpha/2} \end{bmatrix}, \tag{54}$$

and

$$\mathbf{R}_X(\alpha) = \begin{bmatrix} \cos\frac{\alpha}{2} & -i\sin\frac{\alpha}{2} \\ -i\sin\frac{\alpha}{2} & \cos\frac{\alpha}{2} \end{bmatrix}, \tag{55}$$

respectively. The resulting quantum circuit using the controlled-controlled-R_X gates has an intuitive interpretation similar to Ref. [53]; Let us expand $|\psi_0\rangle$ by the computational-basis states $\{|b\rangle\}_{b=0}^{2^{2N_{\text{site}}}-1}$ as $|\psi_0\rangle = \sum_b \langle b|\psi_0\rangle|b\rangle$, where b denotes a bit string of length $2N_{\text{site}}$. The operator $\frac{1}{2}(e^{i\alpha(\hat{n}_{i\uparrow} + \hat{n}_{i\downarrow} - 1)} + e^{-i\alpha(\hat{n}_{i\uparrow} + \hat{n}_{i\downarrow} - 1)}) = \cos(2\alpha\hat{\eta}_i^z)$ applied to $|\psi_0\rangle$ then multiplies a factor $\cos\alpha = e^{-g/2}$ [corresponding to the diagonal element of $\mathbf{R}_X(\pm 2\alpha)$] to basis states $\{|b\rangle\}$ if they are in either doubly occupied configuration $|1\rangle_{i\uparrow}|1\rangle_{i\downarrow}$ or empty configuration $|0\rangle_{i\uparrow}|0\rangle_{i\downarrow}$

(corresponding to the controlled-controlled parts), while it multiplies 1 to the other basis states.

The second approach introduced here can be implemented in a much simpler quantum circuit composed essentially of single-qubit rotation (R_Z) gates without ancillary qubits. However, this approach cannot prepare the Gutzwiller wave function $|\psi_g\rangle$ itself on a quantum computer. Rather, the expectation values of observables are calculated stochastically by the importance sampling. Moreover, in general, the second approach suffers from the phase problem, as does the auxiliary-field quantum Monte Carlo method in classical computation. However, when the phase problem is absent, the second approach can avoid the exponentially hard scaling in the first approach where the success probability $p_{00\cdots 0}$ for preparing the Gutzwiller wave function decreases exponentially in the system size N_{site}. It should be noted that, in the absence of the phase problem, the computational complexity of the auxiliary-field quantum Monte Carlo method in classical computation is already polynomial in N_{site}, thus accessible currently to several hundreds to thousands of sites for Fermi-Hubbard-type models [92–97], and hence the quantum advantage of the second approach is not obvious. However, unlike the auxiliary-field quantum Monte Carlo method, the present approach can be extended to a trial state $|\psi_0\rangle$ that is not an uncorrelated Slater determinant state but a correlated multideterminant state, the latter being prepared, for example, with a variational-quantum-eigensolver scheme. Extension of the present approach to this direction will be worth studying in the future. If the trial state $|\psi_0\rangle$ is spin separable, the corresponding quantum circuit further simplifies as it requires only $N_{\text{site}} + 1$ qubits, as compared to $2N_{\text{site}} + 1$ qubits for the spin-entangled trial state $|\psi_0\rangle$, where "+1" qubit is the ancillary qubit for the Hadamard test.

The present scheme based on the discrete Hubbard-Stratonovich transformation is somewhat similar to the recently proposed method of decomposing a two-qubit unitary gate as a sum of single-qubit gates [98] in the sense that the Gutzwiller factor, corresponding to the two-body interaction, is decomposed into a product of the linear combination of unitary operators, corresponding to one-body terms. A major dif-

TABLE I. Comparison of the gate counts in two quantum circuits proposed in Ref [53] and the present study (see Fig. 1) for probabilistically preparing the Gutzwiller wave function on a quantum computer. The Jordan-Wigner transformation is assumed in both schemes.

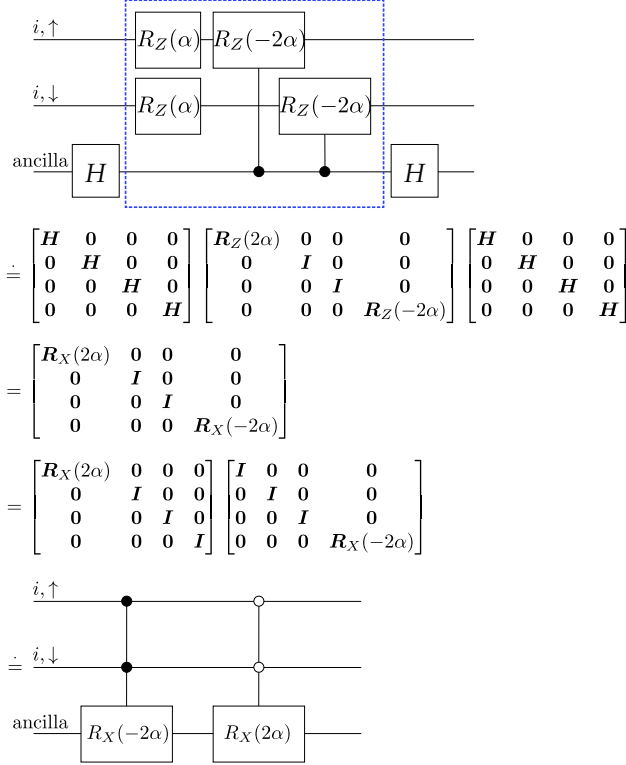|	Ref. [53]	This study
"Unit gate" for implementing the Gutzwiller factor	CCR_Y	$2CR_Z + 2R_Z$
Number of CNOT gates required for decomposing of a single unit gate	12	4
Number of unit gates required for implementing the Gutzwiller factor	N_{site}	N_{site}
Total number of CNOT gates required for implementing the Gutzwiller factor	$12N_{\text{site}}$	$4N_{\text{site}}$

FIG. 8. Different expression of the quantum circuit for taking the linear combination of the one-body operators $\frac{1}{2}(e^{i\alpha(\hat{n}_{i\uparrow}+\hat{n}_{i\downarrow}-1)} + e^{-i\alpha(\hat{n}_{i\uparrow}+\hat{n}_{i\downarrow}-1)})$ with controlled-controlled-unitary gates. The quantum circuit in the first line is the same as that in the lower part of Fig. 1(c). The matrices in the second line (third and fourth lines) are 8×8 matrices, corresponding to the quantum circuit in the first (last) line, with $\mathbf{0}$, $\mathbf{I}$, $\mathbf{H}$, $\mathbf{R}_Z$, and $\mathbf{R}_X$ being the 2×2 null, identity, Hadamard, Z-rotation, and X-rotation matrices, respectively. The diagonal matrix in the second line corresponds to the sequence of the gates enclosed by the blue dotted line in the first line. The matrices are represented with respect to the basis states $|0\rangle_{i_\uparrow}|0\rangle_{i_\downarrow}|0\rangle_{\text{ancilla}}$, $|0\rangle_{i_\uparrow}|0\rangle_{i_\downarrow}|1\rangle_{\text{ancilla}}$, $|0\rangle_{i_\uparrow}|1\rangle_{i_\downarrow}|0\rangle_{\text{ancilla}}$, $\cdots$, $|1\rangle_{i_\uparrow}|1\rangle_{i_\downarrow}|1\rangle_{\text{ancilla}}$.

ference from Ref. [98] is that the Gutzwiller factor is nonunitary and hence no counterparts of the two-qubit unitary gate exist.

The scheme proposed here has several extensions. A straightforward extension is to increase the number of variational parameters by allowing g to be site dependent, i.e., $g \mapsto g_i$, under which the rotation angle α in Eq. (9) becomes site dependent as $\alpha \mapsto \alpha_i = \arccos{(e^{-g_i/2})}$. We also note that the site-dependent chemical potential or "fugacity" fac-

tors in the Gutzwiller factor [99] can also be included if a generalization of the discrete Hubbard-Stratonovich transformation [100] is employed. It is also possible to extend the Gutzwiller factor to the Jastrow operator, which takes into account long-range density-density correlations [101], and to imaginary-time-evolution operators for electron-phonon-coupled systems [102–104], by using different kinds of Hubbard-Stratonovich transformations. A general framework for obtaining discrete Hubbard-Stratonovich transformations of the exponentiated density-density interactions is provided in Appendix A. The research along this line is now in progress.

Appendix A: Discrete Hubbard-Stratonovich transformations

In this Appendix, we provide a general framework for obtaining Hubbard-Stratonovich transformations that transform $e^{-J\hat{Z}_i\hat{Z}_j}$ as a linear combination of unitary operators, both for $J < 0$ and $J > 0$. Since $(\hat{n}_{i\sigma}-\frac{1}{2})(\hat{n}_{j\sigma'}-\frac{1}{2}) \overset{\text{JWT}}{=} \frac{1}{4}\hat{Z}_{i_\sigma}\hat{Z}_{j_{\sigma'}}$, this implies that any exponentiated density-density interactions can be decomposed into a linear combination of unitary operators.

1. $\exp\left(-J\hat{Z}_i\hat{Z}_j\right)$ with $J < 0$

We consider the case of $J = -|J| < 0$. We begin with the matrix representation

$$e^{-J\hat{Z}_i\hat{Z}_j} \doteq \begin{bmatrix} e^{-J} & 0 & 0 & 0 \\ 0 & e^{J} & 0 & 0 \\ 0 & 0 & e^{J} & 0 \\ 0 & 0 & 0 & e^{-J} \end{bmatrix}, \tag{A1}$$

where $e^{-J} > 1$ and $e^{J} < 1$ because $J < 0$. Next, according to Ref. [105], typical two-qubit two-level unitaries have the matrix representations

$$\exp\left[-i\frac{\alpha}{2}\left(\hat{X}_i\hat{X}_j + \hat{Y}_i\hat{Y}_j\right)\right] \doteq \begin{bmatrix} 1 & 0 & 0 & 0 \\ 0 & \cos\alpha & -i\sin\alpha & 0 \\ 0 & -i\sin\alpha & \cos\alpha & 0 \\ 0 & 0 & 0 & 1 \end{bmatrix}, \tag{A2}$$

$$\exp\left[-i\frac{\alpha}{2}\left(\hat{X}_i\hat{Y}_j - \hat{Y}_i\hat{X}_j\right)\right] \doteq \begin{bmatrix} 1 & 0 & 0 & 0 \\ 0 & \cos\alpha & \sin\alpha & 0 \\ 0 & -\sin\alpha & \cos\alpha & 0 \\ 0 & 0 & 0 & 1 \end{bmatrix}, \tag{A3}$$

$$\exp\left[-i\frac{\alpha}{2}\left(\hat{Z}_j - \hat{Z}_i\right)\right] \doteq \begin{bmatrix} 1 & 0 & 0 & 0 \\ 0 & e^{i\alpha} & 0 & 0 \\ 0 & 0 & e^{-i\alpha} & 0 \\ 0 & 0 & 0 & 1 \end{bmatrix}, \tag{A4}$$

where α is real. Since $\sin\alpha$ ($\cos\alpha$) is an odd (even) function of α, linear combinations of these two-qubit two-level unitaries with opposite rotation angles result in a diagonal matrix, i.e.,

$$\sum_{s=\pm 1} \exp\left[-i\frac{s\alpha}{2}\left(\hat{X}_i\hat{X}_j + \hat{Y}_i\hat{Y}_j\right)\right]$$
$$= \sum_{s=\pm 1} \exp\left[-i\frac{s\alpha}{2}\left(\hat{X}_i\hat{Y}_j - \hat{Y}_i\hat{X}_j\right)\right]$$
$$= \sum_{s=\pm 1} \exp\left[-i\frac{s\alpha}{2}\left(\hat{Z}_j - \hat{Z}_i\right)\right]$$
$$\doteq \begin{bmatrix} 2 & 0 & 0 & 0 \\ 0 & 2\cos\alpha & 0 & 0 \\ 0 & 0 & 2\cos\alpha & 0 \\ 0 & 0 & 0 & 2 \end{bmatrix}. \tag{A5}$$

Therefore, comparing Eqs. (A1) and (A5), we find the discrete Hubbard-Stratonovich transformations

$$e^{-J\hat{Z}_i\hat{Z}_j} = \gamma \sum_{s=\pm 1} \exp\left[-i\frac{s\alpha}{2}\left(\hat{X}_i\hat{X}_j + \hat{Y}_i\hat{Y}_j\right)\right] \tag{A6}$$

$$= \gamma \sum_{s=\pm 1} \exp\left[-i\frac{s\alpha}{2}\left(\hat{X}_i\hat{Y}_j - \hat{Y}_i\hat{X}_j\right)\right] \tag{A7}$$

$$= \gamma \sum_{s=\pm 1} \exp\left[-i\frac{s\alpha}{2}\left(\hat{Z}_j - \hat{Z}_i\right)\right] \tag{A8}$$

with $\gamma = e^{-J}/2$ and $\alpha = \arccos\left(e^{2J}\right)$.

2. $\exp\left(-J\hat{Z}_i\hat{Z}_j\right)$ with $J > 0$

Next, we consider the case of $J > 0$, for which $e^{-J} < 1$ and $e^{J} > 1$ in Eq. (A1). According to Ref. [105], typical two-qubit two-level unitaries have the matrix representations

$$\exp\left[-i\frac{\alpha}{2}\left(\hat{X}_i\hat{X}_j - \hat{Y}_i\hat{Y}_j\right)\right] \doteq \begin{bmatrix} \cos\alpha & 0 & 0 & -i\sin\alpha \\ 0 & 1 & 0 & 0 \\ 0 & 0 & 1 & 0 \\ -i\sin\alpha & 0 & 0 & \cos\alpha \end{bmatrix}, \tag{A9}$$

$$\exp\left[-i\frac{\alpha}{2}\left(\hat{X}_i\hat{Y}_j + \hat{Y}_i\hat{X}_j\right)\right] \doteq \begin{bmatrix} \cos\alpha & 0 & 0 & -\sin\alpha \\ 0 & 1 & 0 & 0 \\ 0 & 0 & 1 & 0 \\ \sin\alpha & 0 & 0 & \cos\alpha \end{bmatrix}, \tag{A10}$$

$$\exp\left[-i\frac{\alpha}{2}\left(\hat{Z}_j + \hat{Z}_i\right)\right] \doteq \begin{bmatrix} e^{-i\alpha} & 0 & 0 & 0 \\ 0 & 1 & 0 & 0 \\ 0 & 0 & 1 & 0 \\ 0 & 0 & 0 & e^{i\alpha} \end{bmatrix}, \tag{A11}$$

where α is real. Since $\sin\alpha$ ($\cos\alpha$) is an odd (even) function of α, linear combinations of these two-qubit two-level unitaries with opposite rotation angles result in a diagonal matrix, i.e.,

$$\sum_{s=\pm 1} \exp\left[-i\frac{s\alpha}{2}\left(\hat{X}_i\hat{X}_j - \hat{Y}_i\hat{Y}_j\right)\right]$$
$$= \sum_{s=\pm 1} \exp\left[-i\frac{s\alpha}{2}\left(\hat{X}_i\hat{Y}_j + \hat{Y}_i\hat{X}_j\right)\right]$$
$$= \sum_{s=\pm 1} \exp\left[-i\frac{s\alpha}{2}\left(\hat{Z}_j + \hat{Z}_i\right)\right]$$
$$\doteq \begin{bmatrix} 2\cos\alpha & 0 & 0 & 0 \\ 0 & 2 & 0 & 0 \\ 0 & 0 & 2 & 0 \\ 0 & 0 & 0 & 2\cos\alpha \end{bmatrix}. \tag{A12}$$

Therefore, comparing Eqs. (A1) and (A12), we find the discrete Hubbard-Stratonovich transformations

$$e^{-J\hat{Z}_i\hat{Z}_j} = \gamma \sum_{s=\pm 1} \exp\left[-i\frac{s\alpha}{2}\left(\hat{X}_i\hat{X}_j - \hat{Y}_i\hat{Y}_j\right)\right] \tag{A13}$$

$$= \gamma \sum_{s=\pm 1} \exp\left[-i\frac{s\alpha}{2}\left(\hat{X}_i\hat{Y}_j + \hat{Y}_i\hat{X}_j\right)\right] \tag{A14}$$

$$= \gamma \sum_{s=\pm 1} \exp\left[-i\frac{s\alpha}{2}\left(\hat{Z}_j + \hat{Z}_i\right)\right] \tag{A15}$$

with $\gamma = e^{J}/2$ and $\alpha = \arccos\left(e^{-2J}\right)$.

Equation (A15) corresponds to the discrete Hubbard-Stratonovich transformation in Ref. [59] and is adopted here in this study, while Eqs. (A13) and (A14) are different discrete Hubbard-Stratonovich transformations, which might be useful for other purposes. Finally, we note that Eqs. (A13) and (A14) are similar to the discrete Hubbard-Stratonovich transformation for fermions in anomalous channels discussed in Ref. [106].

Appendix B: Absence of the phase problem

In this Appendix, we prove that the phase problem is absent for our particular case, i.e., $|\psi_0\rangle$ being the ground state of $\hat{K}$ on a bipartite lattice composed of sublattices A and B at half

filling. For this purpose, we introduce a unitary operator $\hat{\mathcal{U}}_{\text{pPH}}$ for the partial particle-hole (pPH) transformation such that

$$\hat{\mathcal{U}}_{\text{pPH}}\hat{c}_{i\uparrow}\hat{\mathcal{U}}_{\text{pPH}}^{-1} = \hat{c}_{i\uparrow}, \tag{B1}$$

$$\hat{\mathcal{U}}_{\text{pPH}}\hat{c}_{i\downarrow}\hat{\mathcal{U}}_{\text{pPH}}^{-1} = (-1)^i \hat{c}_{i\downarrow}^\dagger, \tag{B2}$$

where $(-1)^i$ takes the different sign when site i belongs to the different sublattice on the bipartite lattice. We assume that the number of sites is even. Since $\hat{\mathcal{U}}_{\text{pPH}}\hat{K}\hat{\mathcal{U}}_{\text{pPH}}^{-1} = \hat{K}$ and $\hat{\mathcal{U}}_{\text{pPH}}\hat{D}\hat{\mathcal{U}}_{\text{pPH}}^{-1} = -\hat{D}$, $\hat{K}$ is invariant but $\hat{\mathcal{H}}$ is not invariant under the pPH transformation. Rather, the pPH transformation transforms the repulsive Fermi-Hubbard model to the attractive Fermi-Hubbard model [107]. An explicit form of $\hat{\mathcal{U}}_{\text{pPH}}$ can be written as $\hat{\mathcal{U}}_{\text{pPH}} = \prod_{i=1}^{N_{\text{site}}}(\hat{c}_{i\downarrow} + (-1)^i \hat{c}_{i\downarrow}^\dagger)$ (see for example Refs. [108, 109]).

We also introduce an antiunitary operator $\hat{\mathcal{A}}_{\text{TR}}$ for the time-reversal (TR) operation such that

$$\hat{\mathcal{A}}_{\text{TR}}\hat{c}_{i\uparrow}\hat{\mathcal{A}}_{\text{TR}}^{-1} = \hat{c}_{i\downarrow}, \tag{B3}$$

$$\hat{\mathcal{A}}_{\text{TR}}\hat{c}_{i\downarrow}\hat{\mathcal{A}}_{\text{TR}}^{-1} = -\hat{c}_{i\uparrow}, \tag{B4}$$

and similarly for $\hat{c}_{i\sigma}^\dagger$. The TR operator $\hat{\mathcal{A}}_{\text{TR}}$ can be written as $\hat{\mathcal{A}}_{\text{TR}} = \hat{\mathcal{U}}_{\text{TR}}\hat{C}$, where $\hat{\mathcal{U}}_{\text{TR}}$ is a unitary operator and $\hat{C}$ is the complex-conjugation operator, and hence

$$\hat{\mathcal{A}}_{\text{TR}} z \hat{\mathcal{A}}_{\text{TR}}^{-1} = z^* \tag{B5}$$

for any complex number z. We note that the unitary part $\hat{\mathcal{U}}_{\text{TR}}$ of the TR operator can be explicitly written as $\hat{\mathcal{U}}_{\text{TR}} = \prod_{i=1}^{N_{\text{site}}} \hat{\mathcal{F}}_{i\uparrow,i\downarrow} \mathrm{e}^{\mathrm{i}\pi\hat{n}_{i\downarrow}}$, where $\hat{\mathcal{F}}_{i\sigma,j\sigma'} = 1 + (\hat{c}_{i\sigma}^\dagger \hat{c}_{j\sigma'} + \text{H.c.}) - \hat{c}_{i\sigma}^\dagger \hat{c}_{i\sigma} - \hat{c}_{j\sigma'}^\dagger \hat{c}_{j\sigma'}$ is the fermionic SWAP operator [80, 81, 105, 110–113] and $\mathrm{e}^{\mathrm{i}\phi\hat{n}_{i\downarrow}} = 1 + (\mathrm{e}^{\mathrm{i}\phi} - 1)\hat{n}_{i\downarrow} \overset{\phi=\pi}{=} 1 - 2\hat{n}_{i\downarrow}$ accounts for the gauge transformation [109] for the spin-down fermions in Eq. (B4). From the properties of the fermionic SWAP operator [105] it can be confirmed that $\hat{\mathcal{A}}_{\text{TR}}^2 = \prod_{i=1}^{N_{\text{sites}}}(-1)^{\hat{n}_{i\uparrow}+\hat{n}_{i\downarrow}} = (-1)^{\hat{N}}$. Since $\hat{\mathcal{A}}_{\text{TR}}\hat{K}\hat{\mathcal{A}}_{\text{TR}}^{-1} = \hat{K}$ and $\hat{\mathcal{A}}_{\text{TR}}\hat{D}\hat{\mathcal{A}}_{\text{TR}}^{-1} = \hat{D}$, $\hat{K}$, $\hat{D}$, and hence $\hat{\mathcal{H}}$ are invariant under the TR operation.

For the later convenience, we also introduce another antiunitary operator $\hat{\Theta}$ as $\hat{\Theta} = \hat{\mathcal{U}}_{\text{pPH}}\hat{\mathcal{A}}_{\text{TR}}$. It follows from $\hat{\Theta}\hat{K}\hat{\Theta}^{-1} = \hat{K}$ that, if $|\psi_0\rangle$ is an eigenstate of $\hat{K}$, then $|\tilde{\psi}_0\rangle \equiv \hat{\Theta}|\psi_0\rangle$ is also an eigenstate of $\hat{K}$ with the same eigenvalue. It should be reminded that, if $\hat{\mathcal{A}}$ is an antiunitary operator, $|\psi\rangle$ and $|\phi\rangle$ are some states, and $|\tilde{\psi}\rangle \equiv \hat{\mathcal{A}}|\psi\rangle$ and $|\tilde{\phi}\rangle \equiv \hat{\mathcal{A}}|\phi\rangle$ are the antiunitary-operated states associated with $|\psi\rangle$ and $|\phi\rangle$, respectively, then a matrix element $\langle\psi|\hat{X}|\phi\rangle$ of a linear operator $\hat{X}$ can be written in terms of $|\tilde{\psi}\rangle$ and $|\tilde{\phi}\rangle$ as [114, 115]

$$\langle\psi|\hat{X}|\phi\rangle = \langle\tilde{\phi}|\hat{\mathcal{A}}\hat{X}^\dagger\hat{\mathcal{A}}^{-1}|\tilde{\psi}\rangle. \tag{B6}$$

Now we consider how the operator $\hat{u}_{s,\sigma} \equiv \prod_\tau \hat{u}_{s_\tau,\sigma}$ for a given set of auxiliary fields $s = \{s_{i,\tau}\}$ is transformed by $\hat{\mathcal{U}}_{\text{pPH}}$, $\hat{\mathcal{A}}_{\text{TR}}$, and $\hat{\Theta}$. From Eqs. (B1) and (B2), it follows that

$$\hat{\mathcal{U}}_{\text{pPH}}(\hat{u}_{s,\uparrow} \otimes \hat{u}_{s,\downarrow})\hat{\mathcal{U}}_{\text{pPH}}^{-1} = \hat{u}_{s,\uparrow} \otimes \hat{u}_{s,\downarrow}^*. \tag{B7}$$

From Eqs. (B3), (B4) and (B5), it follows that

$$\hat{\mathcal{A}}_{\text{TR}}(\hat{u}_{s,\uparrow} \otimes \hat{u}_{s,\downarrow})\hat{\mathcal{A}}_{\text{TR}}^{-1} = \hat{u}_{s,\uparrow}^* \otimes \hat{u}_{s,\downarrow}^*. \tag{B8}$$

From Eqs. (B7) and (B8), it follows that

$$\hat{\Theta}(\hat{u}_{s,\uparrow} \otimes \hat{u}_{s,\downarrow})\hat{\Theta}^{-1} = \hat{u}_{s,\uparrow}^* \otimes \hat{u}_{s,\downarrow}. \tag{B9}$$

We also note that $\hat{u}_{s,\sigma}^* = \hat{u}_{s,\sigma}^\dagger$ because $[\hat{u}_{s_\tau,\sigma}, \hat{u}_{s_{\tau'},\sigma}] = 0$.

Next we consider the matrix element

$$W \equiv \langle\psi_0|\hat{u}_{s,\uparrow} \otimes \hat{u}_{s,\downarrow}|\psi_0\rangle, \tag{B10}$$

which corresponds to the numerator of P_s in Eq. (30). Here, we assume that $|\psi_0\rangle$ is the unique ground state of $\hat{K}$, implying that $|\tilde{\psi}_0\rangle = \hat{\Theta}|\psi_0\rangle$ differs from $|\psi_0\rangle$ only by a phase factor, $|\tilde{\psi}_0\rangle = \mathrm{e}^{\mathrm{i}\theta}|\psi_0\rangle$. Note also that $|\psi_0\rangle$ is a spin-separable state. Then, by noticing that $\hat{\Theta}$ is an antiunitary operator, W can be written as

$$\begin{aligned} W &= \langle\tilde{\psi}_0|\hat{\Theta}(\hat{u}_{s,\uparrow} \otimes \hat{u}_{s,\downarrow})^\dagger\hat{\Theta}^{-1}|\tilde{\psi}_0\rangle \\ &= \langle\tilde{\psi}_0|((\hat{u}_{s,\uparrow}^\dagger)^* \otimes \hat{u}_{s,\downarrow}^\dagger)|\tilde{\psi}_0\rangle \\ &= \langle\psi_{0,\uparrow}|(\hat{u}_{s,\uparrow}^*)^\dagger|\psi_{0,\uparrow}\rangle\langle\psi_{0,\downarrow}|\hat{u}_{s,\downarrow}^\dagger|\psi_{0,\downarrow}\rangle \\ &\equiv W_\uparrow W_\downarrow. \end{aligned} \tag{B11}$$

Here, we have used Eq. (B6) in the first equality and Eq. (B9) in the second equality. Since $\hat{\mathcal{A}}_{\text{TR}}\hat{K}_\uparrow\hat{\mathcal{A}}_{\text{TR}}^{-1} = \hat{K}_\downarrow$ and $\hat{\mathcal{A}}_{\text{TR}}\hat{K}_\downarrow\hat{\mathcal{A}}_{\text{TR}}^{-1} = \hat{K}_\uparrow$, we assume that $|\psi_{0,\downarrow}\rangle$ is the time-reversed state of $|\psi_{0,\uparrow}\rangle$, i.e., $|\psi_{0,\downarrow}\rangle = \hat{\mathcal{A}}_{\text{TR}}|\psi_{0,\uparrow}\rangle$ up to a phase factor. Then, by noticing that $\hat{\mathcal{A}}_{\text{TR}}$ is antiunitary, $W_\uparrow$ in Eq. (B11) can be written as

$$\begin{aligned} W_\uparrow &= \langle\psi_{0,\downarrow}|\hat{\mathcal{A}}_{\text{TR}}\hat{u}_{s,\uparrow}^*\hat{\mathcal{A}}_{\text{TR}}^{-1}|\psi_{0,\downarrow}\rangle \\ &= \langle\psi_{0,\downarrow}|\hat{u}_{s,\downarrow}|\psi_{0,\downarrow}\rangle \\ &= W_\downarrow^*. \end{aligned} \tag{B12}$$

Therefore, $W = |W_\downarrow|^2 > 0$, proving that the phase problem is absent in this case. This is essentially the same argument used to prove the absence of the negative sign problem for the Fermi-Hubbard model in the auxiliary-field quantum Monte-Carlo method [116–118].

---

[1] H. Fehske, R. Schneider, and A Weiße, eds., Computational Many-Particle Physics, Lect. Notes Phys. 739 (Springer, Berlin Heidelberg, 2008).

[2] Richard P. Feynman, "Simulating physics with computers," International Journal of Theoretical Physics **21**, 467–488 (1982).

[3] Y. Nakamura, Yu A. Pashkin, and J. S. Tsai, "Coherent control of macroscopic quantum states in a single-Cooper-pair box," Nature **398**, 786–788 (1999).

[4] Pieter Kok, W. J. Munro, Kae Nemoto, T. C. Ralph, Jonathan P. Dowling, and G. J. Milburn, "Linear optical quantum computing with photonic qubits," Rev. Mod. Phys. **79**, 135–174 (2007).

[5] T. D. Ladd, F. Jelezko, R. Laflamme, Y. Nakamura, C. Monroe, and J. L. O'Brien, "Quantum computers," Nature **464**, 45–53 (2010).

[6] Ze-Liang Xiang, Sahel Ashhab, J. Q. You, and Franco Nori, "Hybrid quantum circuits: Superconducting circuits interacting with other quantum systems," Rev. Mod. Phys. **85**, 623–653 (2013).

[7] Jerry M. Chow, Jay M. Gambetta, Easwar Magesan, David W. Abraham, Andrew W. Cross, B. R. Johnson, Nicholas A. Masluk, Colm A. Ryan, John A. Smolin, Srikanth J. Srinivasan, and M. Steffen, "Implementing a strand of a scalable fault-tolerant quantum computing fabric," Nature Communications **5**, 4015 (2014).

[8] R. Barends, J. Kelly, A. Megrant, A. Veitia, D. Sank, E. Jeffrey, T. C. White, J. Mutus, A. G. Fowler, B. Campbell, Y. Chen, Z. Chen, B. Chiaro, A. Dunsworth, C. Neill, P. O'Malley, P. Roushan, A. Vainsencher, J. Wenner, A. N. Korotkov, A. N. Cleland, and John M. Martinis, "Superconducting quantum circuits at the surface code threshold for fault tolerance," Nature **508**, 500–503 (2014).

[9] D. Ristè, S. Poletto, M.-Z. Huang, A. Bruno, V. Vesterinen, O.-P. Saira, and L. DiCarlo, "Detecting bit-flip errors in a logical qubit using stabilizer measurements," Nature Communications **6**, 6983 (2015).

[10] J. Kelly, R. Barends, A. G. Fowler, A. Megrant, E. Jeffrey, T. C. White, D. Sank, J. Y. Mutus, B. Campbell, Yu Chen, Z. Chen, B. Chiaro, A. Dunsworth, I.-C. Hoi, C. Neill, P. J. J. O'Malley, C. Quintana, P. Roushan, A. Vainsencher, J. Wenner, A. N. Cleland, and John M. Martinis, "State preservation by repetitive error detection in a superconducting quantum circuit," Nature **519**, 66–69 (2015).

[11] Frank Arute, Kunal Arya, Ryan Babbush, Dave Bacon, Joseph C. Bardin, Rami Barends, Rupak Biswas, Sergio Boixo, Fernando G. S. L. Brandao, David A. Buell, Brian Burkett, Yu Chen, Zijun Chen, Ben Chiaro, Roberto Collins, William Courtney, Andrew Dunsworth, Edward Farhi, Brooks Foxen, Austin Fowler, Craig Gidney, Marissa Giustina, Rob Graff, Keith Guerin, Steve Habegger, Matthew P. Harrigan, Michael J. Hartmann, Alan Ho, Markus Hoffmann, Trent Huang, Travis S. Humble, Sergei V. Isakov, Evan Jeffrey, Zhang Jiang, Dvir Kafri, Kostyantyn Kechedzhi, Julian Kelly, Paul V. Klimov, Sergey Knysh, Alexander Korotkov, Fedor Kostritsa, David Landhuis, Mike Lindmark, Erik Lucero, Dmitry Lyakh, Salvatore Mandrà, Jarrod R. McClean, Matthew McEwen, Anthony Megrant, Xiao Mi, Kristel Michielsen, Masoud Mohseni, Josh Mutus, Ofer Naaman, Matthew Neeley, Charles Neill, Murphy Yuezhen Niu, Eric Ostby, Andre Petukhov, John C. Platt, Chris Quintana, Eleanor G. Rieffel, Pedram Roushan, Nicholas C. Rubin, Daniel Sank, Kevin J. Satzinger, Vadim Smelyanskiy, Kevin J. Sung, Matthew D. Trevithick, Amit Vainsencher, Benjamin Villalonga, Theodore White, Z. Jamie Yao, Ping Yeh, Adam Zalcman, Hartmut Neven, and John M. Martinis, "Quantum supremacy using a programmable superconducting processor," Nature **574**, 505–510 (2019).

[12] Han-Sen Zhong, Hui Wang, Yu-Hao Deng, Ming-Cheng Chen, Li-Chao Peng, Yi-Han Luo, Jian Qin, Dian Wu, Xing Ding, Yi Hu, Peng Hu, Xiao-Yan Yang, Wei-Jun Zhang, Hao Li, Yuxuan Li, Xiao Jiang, Lin Gan, Guangwen Yang, Lixing You, Zhen Wang, Li Li, Nai-Le Liu, Chao-Yang Lu, and Jian-Wei Pan, "Quantum computational advantage using photons," Science **370**, 1460–1463 (2020).

[13] M.-H. Yung, J. Casanova, A. Mezzacapo, J. McClean, L. Lamata, A. Aspuru-Guzik, and E. Solano, "From transistor to trapped-ion computers for quantum chemistry," Scientific Reports **4**, 3589 (2014).

[14] Alberto Peruzzo, Jarrod McClean, Peter Shadbolt, Man-Hong Yung, Xiao-Qi Zhou, Peter J. Love, Alán Aspuru-Guzik, and Jeremy L. O'Brien, "A variational eigenvalue solver on a photonic quantum processor," Nature Communications **5**, 4213 (2014).

[15] Dave Wecker, Matthew B. Hastings, and Matthias Troyer, "Progress towards practical quantum variational algorithms," Phys. Rev. A **92**, 042303 (2015).

[16] P. J. J. O'Malley, R. Babbush, I. D. Kivlichan, J. Romero, J. R. McClean, R. Barends, J. Kelly, P. Roushan, A. Tranter, N. Ding, B. Campbell, Y. Chen, Z. Chen, B. Chiaro, A. Dunsworth, A. G. Fowler, E. Jeffrey, E. Lucero, A. Megrant, J. Y. Mutus, M. Neeley, C. Neill, C. Quintana, D. Sank, A. Vainsencher, J. Wenner, T. C. White, P. V. Coveney, P. J. Love, H. Neven, A. Aspuru-Guzik, and J. M. Martinis, "Scalable Quantum Simulation of Molecular Energies," Phys. Rev. X **6**, 031007 (2016).

[17] Jarrod R. McClean, Jonathan Romero, Ryan Babbush, and Alán Aspuru-Guzik, "The theory of variational hybrid quantum-classical algorithms," New Journal of Physics **18**, 023023 (2016).

[18] Abhinav Kandala, Antonio Mezzacapo, Kristan Temme, Maika Takita, Markus Brink, Jerry M. Chow, and Jay M. Gambetta, "Hardware-efficient variational quantum eigensolver for small molecules and quantum magnets," Nature **549**, 242 (2017).

[19] Jun Li, Xiaodong Yang, Xinhua Peng, and Chang-Pu Sun, "Hybrid Quantum-Classical Approach to Quantum Optimal Control," Phys. Rev. Lett. **118**, 150503 (2017).

[20] Guglielmo Mazzola, Pauline J. Ollitrault, Panagiotis Kl. Barkoutsos, and Ivano Tavernelli, "Nonunitary operations for ground-state calculations in near-term quantum computers," Phys. Rev. Lett. **123**, 130501 (2019).

[21] Frank Arute, Kunal Arya, Ryan Babbush, Dave Bacon, Joseph C. Bardin, Rami Barends, Sergio Boixo, Michael Broughton, Bob B. Buckley, David A. Buell, Brian Burkett, Nicholas Bushnell, Yu Chen, Zijun Chen, Benjamin Chiaro, Roberto Collins, William Courtney, Sean Demura, Andrew Dunsworth, Edward Farhi, Austin Fowler, Brooks Foxen, Craig Gidney, Marissa Giustina, Rob Graff, Steve Habegger, Matthew P. Harrigan, Alan Ho, Sabrina Hong, Trent Huang, William J. Huggins, Lev Ioffe, Sergei V. Isakov, Evan Jeffrey, Zhang Jiang, Cody Jones, Dvir Kafri, Kostyantyn Kechedzhi, Julian Kelly, Seon Kim, Paul V. Klimov, Alexander Korotkov, Fedor Kostritsa, David Landhuis, Pavel Laptev, Mike Lindmark, Erik Lucero, Orion Martin, John M. Martinis, Jarrod R. McClean, Matt McEwen, Anthony Megrant, Xiao Mi, Masoud Mohseni, Wojciech Mruczkiewicz, Josh Mutus, Ofer Naaman, Matthew Neeley, Charles Neill, Hartmut Neven, Murphy Yuezhen Niu, Thomas E. O'Brien, Eric Ostby, Andre Petukhov, Harald Putterman, Chris Quintana, Pedram Roushan, Nicholas C. Rubin, Daniel Sank, Kevin J. Satzinger, Vadim Smelyanskiy, Doug Strain, Kevin J. Sung, Marco Szalay, Tyler Y. Takeshita, Amit Vainsencher, Theodore White, Nathan Wiebe, Z. Jamie Yao, Ping Yeh, and Adam Zalcman, "Hartree-Fock on a superconducting qubit quantum computer," Science **369**, 1084–1089 (2020), https://science.sciencemag.org/content/369/6507/1084.full.pdf.

[22] Philippe Suchsland, Panagiotis Kl. Barkoutsos, Ivano Tavernelli, Mark H. Fischer, and Titus Neupert, "Simulating a ring-like Hubbard system with a quantum computer," Phys. Rev. Research 4, 013165 (2022).

[23] Stasja Stanisic, Jan Lukas Bosse, Filippo Maria Gambetta, Raul A. Santos, Wojciech Mruczkiewicz, Thomas E. O'Brien, Eric Ostby, and Ashley Montanaro, "Observing ground-state properties of the Fermi-Hubbard model using a scalable algorithm on a quantum computer," (2021), arXiv:2112.02025 [quant-ph].

[24] Jarrod R. McClean, Mollie E. Kimchi-Schwartz, Jonathan Carter, and Wibe A. de Jong, "Hybrid quantum-classical hierarchy for mitigation of decoherence and determination of excited states," Phys. Rev. A 95, 042308 (2017).

[25] J. I. Colless, V. V. Ramasesh, D. Dahlen, M. S. Blok, M. E. Kimchi-Schwartz, J. R. McClean, J. Carter, W. A. de Jong, and I. Siddiqi, "Computation of Molecular Spectra on a Quantum Processor with an Error-Resilient Algorithm," Phys. Rev. X 8, 011021 (2018).

[26] Robert M. Parrish, Edward G. Hohenstein, Peter L. McMahon, and Todd J. Martínez, "Quantum Computation of Electronic Transitions Using a Variational Quantum Eigensolver," Phys. Rev. Lett. 122, 230401 (2019).

[27] Ken M. Nakanishi, Kosuke Mitarai, and Keisuke Fujii, "Subspace-search variational quantum eigensolver for excited states," Phys. Rev. Research 1, 033062 (2019).

[28] Kentaro Heya, Ken M Nakanishi, Kosuke Mitarai, and Keisuke Fujii, "Subspace Variational Quantum Simulator," (2019), arXiv:1904.08566 [quant-ph].

[29] William J Huggins, Joonho Lee, Unpil Baek, Bryan O'Gorman, and K Birgitta Whaley, "A non-orthogonal variational quantum eigensolver," New Journal of Physics 22, 073009 (2020).

[30] John Preskill, "Quantum Computing in the NISQ era and beyond," Quantum 2, 79 (2018).

[31] Sam McArdle, Suguru Endo, Alán Aspuru-Guzik, Simon C. Benjamin, and Xiao Yuan, "Quantum computational chemistry," Rev. Mod. Phys. 92, 015003 (2020).

[32] Suguru Endo, Zhenyu Cai, Simon C. Benjamin, and Xiao Yuan, "Hybrid quantum-classical algorithms and quantum error mitigation," Journal of the Physical Society of Japan 90, 032001 (2021).

[33] M. Cerezo, Andrew Arrasmith, Ryan Babbush, Simon C. Benjamin, Suguru Endo, Keisuke Fujii, Jarrod R. McClean, Kosuke Mitarai, Xiao Yuan, Lukasz Cincio, and Patrick J. Coles, "Variational quantum algorithms," Nature Reviews Physics 3, 625–644 (2021).

[34] Jules Tilly, Hongxiang Chen, Shuxiang Cao, Dario Picozzi, Kanav Setia, Ying Li, Edward Grant, Leonard Wossnig, Ivan Rungger, George H. Booth, and Jonathan Tennyson, "The variational quantum eigensolver: a review of methods and best practices," (2021), arXiv:2111.05176 [quant-ph].

[35] Kazuhiro Seki, Tomonori Shirakawa, and Seiji Yunoki, "Symmetry-adapted variational quantum eigensolver," Phys. Rev. A 101, 052340 (2020).

[36] Martin C. Gutzwiller, "Effect of correlation on the ferromagnetism of transition metals," Phys. Rev. Lett. 10, 159–162 (1963).

[37] Dieter Vollhardt, "Normal ^{3}He: an almost localized Fermi liquid," Rev. Mod. Phys. 56, 99–120 (1984).

[38] P. W. Anderson, "The Resonating Valence Bond State in La_2CuO_4 and Superconductivity," Science 235, 1196–1198 (1987).

[39] A. Himeda and M. Ogata, "Spontaneous deformation of the fermi surface due to strong correlation in the two-dimensional t- J model," Phys. Rev. Lett. 85, 4345–4348 (2000).

[40] Masao Ogata and Akihiro Himeda, "Superconductivity and Antiferromagnetism in an Extended Gutzwiller Approximation for t-J Model: Effect of Double-Occupancy Exclusion," Journal of the Physical Society of Japan 72, 374–391 (2003).

[41] Michele Fabrizio, "Gutzwiller description of non-magnetic mott insulators: Dimer lattice model," Phys. Rev. B 76, 165110 (2007).

[42] F. D. M. Haldane, "Exact Jastrow-Gutzwiller resonating-valence-bond ground state of the spin-$\frac{1}{2}$ antiferromagnetic Heisenberg chain with $1/r^2$ exchange," Phys. Rev. Lett. 60, 635–638 (1988).

[43] B. Sriram Shastry, "Exact solution of an $S = 1/2$ Heisenberg antiferromagnetic chain with long-ranged interactions," Phys. Rev. Lett. 60, 639–642 (1988).

[44] Hisatoshi Yokoyama and Hiroyuki Shiba, "Hubbard Model in Strong Correlation Regime –Variational Monte-Carlo Studies on Singlet Liquid and Néel State–," Journal of the Physical Society of Japan 56, 3570–3581 (1987).

[45] Y. Kuramoto and H. Yokoyama, "Exactly soluble supersymmetric t-J-type model with long-range exchange and transfer," Phys. Rev. Lett. 67, 1338–1341 (1991).

[46] Hisatoshi Yokoyama and Masao Ogata, "Variational wave functions and ground-state properties in the one-dimensional t-J model," Phys. Rev. Lett. 67, 3610–3613 (1991).

[47] A. Himeda, T. Kato, and M. Ogata, "Stripe States with Spatially Oscillating d-Wave Superconductivity in the Two-Dimensional t-t′-J Model," Phys. Rev. Lett. 88, 117001 (2002).

[48] Seiji Yunoki, "Coherent inverse photoemission spectrum for gutzwiller projected superconductors," Phys. Rev. B 72, 092505 (2005).

[49] Patrick A. Lee, Naoto Nagaosa, and Xiao-Gang Wen, "Doping a mott insulator: Physics of high-temperature superconductivity," Rev. Mod. Phys. 78, 17–85 (2006).

[50] Seiji Yunoki, "Single-particle anomalous excitations of Gutzwiller-projected BCS superconductors and Bogoliubov quasiparticle characteristics," Phys. Rev. B 74, 180504 (2006).

[51] Shengtao Jiang, Douglas J. Scalapino, and Steven R. White, "Ground-state phase diagram of the t-t′-J model," Proceedings of the National Academy of Sciences 118, e2109978118 (2021).

[52] Yongxin Yao, Feng Zhang, Cai-Zhuang Wang, Kai-Ming Ho, and Peter P. Orth, "Gutzwiller hybrid quantum-classical computing approach for correlated materials," Phys. Rev. Research 3, 013184 (2021).

[53] Bruno Murta and J. Fernández-Rossier, "Gutzwiller wave function on a digital quantum computer," Phys. Rev. B 103, L241113 (2021).

[54] Robert Jastrow, "Many-body problem with strong forces," Phys. Rev. 98, 1479–1484 (1955).

[55] Manuela Capello, Federico Becca, Michele Fabrizio, Sandro Sorella, and Erio Tosatti, "Variational Description of Mott Insulators," Phys. Rev. Lett. 94, 026406 (2005).

[56] Robert M. Gingrich and Colin P. Williams, "Non-unitary probabilistic quantum computing," in Proceedings of the Winter International Synposium on Information and Communication, WISICT '04 (Trinity College Dublin, 2004) pp. 1–6.

[57] Tong Liu, Jin-Guo Liu, and Heng Fan, "Probabilistic nonunitary gate in imaginary time evolution," Quantum Information Processing 20, 204 (2021).

[58] Taichi Kosugi, Yusuke Nishiya, and Yu ichiro Matsushita, "Probabilistic imaginary-time evolution by using forward and

backward real-time evolution with a single ancilla: first-quantized eigensolver of quantum chemistry for ground states," (2021), arXiv:2111.12471 [quant-ph].

[59] J. E. Hirsch, "Discrete Hubbard-Stratonovich transformation for fermion lattice models," Phys. Rev. B **28**, 4059–4061 (1983).

[60] J. Hubbard, "Calculation of partition functions," Phys. Rev. Lett. **3**, 77–78 (1959).

[61] F. Gebhard, The Mott Metal-Insulator Transition, Vol. 137 (Springer, Berlin, 1997) Chap. 3.

[62] Hisatoshi Yokoyama and Hiroyuki Shiba, "Variational Monte-Carlo Studies of Hubbard Model. I," Journal of the Physical Society of Japan **56**, 1490–1506 (1987).

[63] Note however that $e^{-2g\hat{D}}$ in the denominator in Eq. (13) can also be decomposed directly without introducing the two kinds of auxiliary fields $\{s_{i,\tau}\}$ with $\tau = 1, 2$.

[64] F. Assaad and H Evertz, Computational Many-Particle Physics, Vol. 739 (Springer Berlin Heidelberg, Berlin, Heidelberg, 2008) pp. 277–356.

[65] F. Becca and S. Sorella, Quantum Monte Carlo Approaches for Correlated Systems (Cambridge University Press, Cambridge, 2017).

[66] Kazuhiro Seki and Seiji Yunoki, "Quantum Power Method by a Superposition of Time-Evolved States," PRX Quantum **2**, 010333 (2021).

[67] Andrew M. Childs and Nathan Weibe, "Hamiltonian simulation using linear combinations of unitary operations," Quantum Information and Computation **12**, 901 (2012).

[68] Taichi Kosugi and Yuichiro Matsushita, "Construction of green's functions on a quantum computer: Quasiparticle spectra of molecules," Phys. Rev. A **101**, 012330 (2020).

[69] C. Gros, R. Joynt, and T. M. Rice, "Antiferromagnetic correlations in almost-localized Fermi liquids," Phys. Rev. B **36**, 381–393 (1987).

[70] A. Brooks Harris and Robert V. Lange, "Single-particle excitations in narrow energy bands," Phys. Rev. **157**, 295–314 (1967).

[71] J. E. Hirsch, "Attractive interaction and pairing in fermion systems with strong on-site repulsion," Phys. Rev. Lett. **54**, 1317–1320 (1985).

[72] F. C. Zhang and T. M. Rice, "Effective Hamiltonian for the superconducting Cu oxides," Phys. Rev. B **37**, 3759–3761 (1988).

[73] Henk Eskes, Andrzej M. Oleś, Marcel B. J. Meinders, and Walter Stephan, "Spectral properties of the Hubbard bands," Phys. Rev. B **50**, 17980–18002 (1994).

[74] Henk Eskes and Robert Eder, "Hubbard model versus $t - J$ model: The one-particle spectrum," Phys. Rev. B **54**, R14226–R14229 (1996).

[75] Y. Otsuka, Y. Morita, and Y. Hatsugai, "Anisotropy on the Fermi surface of the two-dimensional Hubbard model," Phys. Rev. B **66**, 073109 (2002).

[76] R. Eder, K. Seki, and Y. Ohta, "Self-energy and Fermi surface of the two-dimensional Hubbard model," Phys. Rev. B **83**, 205137 (2011).

[77] Masatoshi Imada and Yasuhiro Hatsugai, "Numerical Studies on the Hubbard Model and the $t - J$ Model in One- and Two-Dimensions," Journal of the Physical Society of Japan **58**, 3752–3780 (1989).

[78] E. Y. Loh, J. E. Gubernatis, R. T. Scalettar, S. R. White, D. J. Scalapino, and R. L. Sugar, "Sign problem in the numerical simulation of many-electron systems," Phys. Rev. B **41**, 9301–9307 (1990).

[79] D. R. Hamann and S. B. Fahy, "Energy measurement in auxiliary-field many-electron calculations," Phys. Rev. B **41**, 11352–11363 (1990).

[80] Dave Wecker, Matthew B. Hastings, Nathan Wiebe, Bryan K. Clark, Chetan Nayak, and Matthias Troyer, "Solving strongly correlated electron models on a quantum computer," Phys. Rev. A **92**, 062318 (2015).

[81] Ian D. Kivlichan, Jarrod McClean, Nathan Wiebe, Craig Gidney, Alán Aspuru-Guzik, Garnet Kin-Lic Chan, and Ryan Babbush, "Quantum Simulation of Electronic Structure with Linear Depth and Connectivity," Phys. Rev. Lett. **120**, 110501 (2018).

[82] Zhang Jiang, Kevin J. Sung, Kostyantyn Kechedzhi, Vadim N. Smelyanskiy, and Sergio Boixo, "Quantum Algorithms to Simulate Many-Body Physics of Correlated Fermions," Phys. Rev. Applied **9**, 044036 (2018).

[83] Tomonori Shirakawa, Kazuhiro Seki, and Seiji Yunoki, "Discretized quantum adiabatic process for free fermions and comparison with the imaginary-time evolution," Phys. Rev. Research **3**, 013004 (2021).

[84] Kosuke Mitarai and Keisuke Fujii, "Methodology for replacing indirect measurements with direct measurements," Phys. Rev. Res. **1**, 013006 (2019).

[85] Francesco Tacchino, Alessandro Chiesa, Stefano Carretta, and Dario Gerace, "Quantum Computers as Universal Quantum Simulators: State-of-the-Art and Perspectives," Adv. Quantum Technol. **3**, 1900052 (2020).

[86] MD SAJID ANIS, Héctor Abraham, AduOffei, Rochisha Agarwal, Gabriele Agliardi, Merav Aharoni, Ismail Yunus Akhalwaya, Gadi Aleksandrowicz, Thomas Alexander, Matthew Amy, Sashwat Anagolum, Eli Arbel, Abraham Asfaw, Anish Athalye, Artur Avkhadiev, Carlos Azaustre, PRATHAMESH BHOLE, Abhik Banerjee, Santanu Banerjee, Will Bang, Aman Bansal, Panagiotis Barkoutsos, Ashish Barnawal, George Barron, George S. Barron, Luciano Bello, Yael Ben-Haim, Daniel Bevenius, Dhruv Bhatnagar, Arjun Bhobe, Paolo Bianchini, Lev S. Bishop, Carsten Blank, Sorin Bolos, Soham Bopardikar, Samuel Bosch, Sebastian Brandhofer, Brandon, Sergey Bravyi, Nick Bronn, Bryce-Fuller, David Bucher, Artemiy Burov, Fran Cabrera, Padraic Calpin, Lauren Capelluto, Jorge Carballo, Ginés Carrascal, Adam Carriker, Ivan Carvalho, Adrian Chen, Chun-Fu Chen, Edward Chen, Jielun (Chris) Chen, Richard Chen, Franck Chevallier, Kartik Chinda, Rathish Cholarajan, Jerry M. Chow, Spencer Churchill, Christian Claus, Christian Clauss, Caleb Clothier, Romilly Cocking, Ryan Cocuzzo, Jordan Connor, Filipe Correa, Abigail J. Cross, Andrew W. Cross, Simon Cross, Juan Cruz-Benito, Chris Culver, Antonio D. Córcoles-Gonzales, Navaneeth D, Sean Dague, Tareq El Dandachi, Animesh N Dangwal, Jonathan Daniel, Marcus Daniels, Matthieu Dartiailh, Abdón Rodríguez Davila, Faisal Debouni, Anton Dekusar, Amol Deshmukh, Mohit Deshpande, Delton Ding, Jun Doi, Eli M. Dow, Eric Drechsler, Eugene Dumitrescu, Karel Dumon, Ivan Duran, Kareem EL-Safty, Eric Eastman, Grant Eberle, Amir Ebrahimi, Pieter Eendebak, Daniel Egger, ElePT, Emilio, Alberto Espiricueta, Mark Everitt, Davide Facoetti, Farida, Paco Martín Fernández, Samuele Ferracin, Davide Ferrari, Axel Hernández Ferrera, Romain Fouilland, Albert Frisch, Andreas Fuhrer, Bryce Fuller, MELVIN GEORGE, Julien Gacon, Borja Godoy Gago, Claudio Gambella, Jay M. Gambetta, Adhisha Gammanpila, Luis Garcia, Tanya Garg, Shelly Garion, Tim Gates, Leron Gil, Austin Gilliam, Aditya Giridharan, Juan Gomez-Mosquera, Gonzalo, Salvador de la Puente González, Jesse Gorzinski, Ian Gould, Donny Greenberg, Dmitry Grinko, Wen Guan, John A.

Gunnels, Harshit Gupta, Naman Gupta, Jakob M. Günther, Mikael Haglund, Isabel Haide, Ikko Hamamura, Omar Costa Hamido, Frank Harkins, Areeq Hasan, Vojtech Havlicek, Joe Hellmers, Łukasz Herok, Stefan Hillmich, Hiroshi Horii, Connor Howington, Shaohan Hu, Wei Hu, Junye Huang, Rolf Huisman, Haruki Imai, Takashi Imamichi, Kazuaki Ishizaki, Ishwor, Raban Iten, Toshinari Itoko, Alexander Ivrii, Ali Javadi, Ali Javadi-Abhari, Wahaj Javed, Qian Jianhua, Madhav Jivrajani, Kiran Johns, Scott Johnstun, Jonathan-Shoemaker, JosDenmark, JoshDumo, John Judge, Tal Kachmann, Akshay Kale, Naoki Kanazawa, Jessica Kane, Kang-Bae, Annanay Kapila, Anton Karazeev, Paul Kassebaum, Josh Kelso, Scott Kelso, Vismai Khanderao, Spencer King, Yuri Kobayashi, Kovi11Day, Arseny Kovyrshin, Rajiv Krishnakumar, Vivek Krishnan, Kevin Krsulich, Prasad Kumkar, Gawel Kus, Ryan LaRose, Enrique Lacal, Raphaël Lambert, Haggai Landa, John Lapeyre, Joe Latone, Scott Lawrence, Christina Lee, Gushu Li, Jake Lishman, Dennis Liu, Peng Liu, Yunho Maeng, Saurav Maheshkar, Kahan Majmudar, Aleksei Malyshev, Mohamed El Mandouh, Joshua Manela, Manjula, Jakub Marecek, Manoel Marques, Kunal Marwaha, Dmitri Maslov, Paweł Maszota, Dolph Mathews, Atsushi Matsuo, Farai Mazhandu, Doug McClure, Maureen McElaney, Cameron McGarry, David McKay, Dan McPherson, Srujan Meesala, Dekel Meirom, Corey Mendell, Thomas Metcalfe, Martin Mevissen, Andrew Meyer, Antonio Mezzacapo, Rohit Midha, Daniel Miller, Zlatko Minev, Abby Mitchell, Nikolaj Moll, Alejandro Montanez, Gabriel Monteiro, Michael Duane Mooring, Renier Morales, Niall Moran, David Morcuende, Seif Mostafa, Mario Motta, Romain Moyard, Prakash Murali, Jan Müggenburg, David Nadlinger, Ken Nakanishi, Giacomo Nannicini, Paul Nation, Edwin Navarro, Yehuda Naveh, Scott Wyman Neagle, Patrick Neuweiler, Aziz Ngoueya, Johan Nicander, Nick-Singstock, Pradeep Niroula, Hassi Norlen, NuoWenLei, Lee James O'Riordan, Oluwatobi Ogunbayo, Pauline Ollitrault, Tamiya Onodera, Raul Otaolea, Steven Oud, Dan Padilha, Hanhee Paik, Soham Pal, Yuchen Pang, Ashish Panigrahi, Vincent R. Pascuzzi, Simone Perriello, Eric Peterson, Anna Phan, Francesco Piro, Marco Pistoia, Christophe Piveteau, Julia Plewa, Pierre Pocreau, Alejandro Pozas-Kerstjens, Rafał Pracht, Milos Prokop, Viktor Prutyanov, Sumit Puri, Daniel Puzzuoli, Jesús Pérez, Quant02, Quintiii, Isha R, Rafey Iqbal Rahman, Arun Raja, Roshan Rajeev, Nipun Ramagiri, Anirudh Rao, Rudy Raymond, Oliver Reardon-Smith, Rafael Martín-Cuevas Redondo, Max Reuter, Julia Rice, Matt Riedemann, Rietesh, Drew Risinger, Marcello La Rocca, Diego M. Rodríguez, RohithKarur, Ben Rosand, Max Rossmannek, Mingi Ryu, Tharrmashastha SAPV, Nahum Rosa Cruz Sa, Arijit Saha, Abdullah Ash-Saki, Sankalp Sanand, Martin Sandberg, Hirmay Sandesara, Ritvik Sapra, Hayk Sargsyan, Aniruddha Sarkar, Ninad Sathaye, Bruno Schmitt, Chris Schnabel, Zachary Schoenfeld, Travis L. Scholten, Eddie Schoute, Mark Schulterbrandt, Joachim Schwarm, James Seaward, Sergi, Ismael Faro Sertage, Kanav Setia, Freya Shah, Nathan Shammah, Rohan Sharma, Yunong Shi, Jonathan Shoemaker, Adenilton Silva, Andrea Simonetto, Divyanshu Singh, Parmeet Singh, Phattharaporn Singkanipa, Yukio Siraichi, Siri, Jesús Sistos, Iskandar Sitdikov, Seyon Sivarajah, Magnus Berg Sletfjerding, John A. Smolin, Mathias Soeken, Igor Olegovich Sokolov, Igor Sokolov, Vicente P. Soloviev, SooluThomas, Starfish, Dominik Steenken, Matt Stypulkoski, Adrien Suau, Shaojun Sun, Kevin J. Sung, Makoto Suwama, Oskar Słowik, Hitomi Takahashi, Tanvesh Takawale, Ivano Tavernelli, Charles Taylor, Pete Tay-

lour, Soolu Thomas, Kevin Tian, Mathieu Tillet, Maddy Tod, Miroslav Tomasik, Caroline Tornow, Enrique de la Torre, Juan Luis Sánchez Toural, Kenso Trabing, Matthew Treinish, Dimitar Trenev, TrishaPe, Felix Truger, Georgios Tsilimigkounakis, Davindra Tulsi, Wes Turner, Yotam Vaknin, Carmen Recio Valcarce, Francois Varchon, Adish Vartak, Almudena Carrera Vazquez, Prajjwal Vijaywargiya, Victor Villar, Bhargav Vishnu, Desiree Vogt-Lee, Christophe Vuillot, James Weaver, Johannes Weidenfeller, Rafal Wieczorek, Jonathan A. Wildstrom, Jessica Wilson, Erick Winston, WinterSoldier, Jack J. Woehr, Stefan Woerner, Ryan Woo, Christopher J. Wood, Ryan Wood, Steve Wood, James Wootton, Matt Wright, Lucy Xing, Bo Yang, Daniyar Yeralin, Ryota Yonekura, David Yonge-Mallo, Ryuhei Yoshida, Richard Young, Jessie Yu, Lebin Yu, Christopher Zachow, Laura Zdanski, Helena Zhang, Christa Zoufal, aeddins ibm, alexzhang13, b63, bartek bartlomiej, bcamorrison, brandhsn, charmerDark, deeplokhande, dekel.meirom, dime10, dlasecki, ehchen, fanizzamarco, fs1132429, gadial, galeinston, georgezhou20, georgios ts, gruu, hhorii, hykavitha, itoko, jessica angel7, jliu45, jscott2, klinvill, krutik2966, ma5x, michelle4654, msuwama, ntgiwsvp, ordmoj, sagar pahwa, pritamsinha2304, ryancocuzzo, saswati qiskit, septembrr, sethmerkel, shaashwat, sternparky, strickroman, tigerjack, tsura crisaldo, vadebayo49, welien, willhbang, wmurphy collabstar, yang.luh, and Mantas Čepulkovskis, "Qiskit: An open-source framework for quantum computing," (2021).

[87] IBM, "Ibm quantum," https://quantum-computing.ibm.com.

[88] A. Chiesa, F. Tacchino, M. Grossi, P. Santini, I. Tavernelli, D. Gerace, and S. Carretta, "Quantum hardware simulating four-dimensional inelastic neutron scattering," Nature Physics 15, 455 (2019).

[89] Akhil Francis, J. K. Freericks, and A. F. Kemper, "Quantum computation of magnon spectra," Phys. Rev. B 101, 1 (2020).

[90] Adriano Barenco, Charles H. Bennett, Richard Cleve, David P. DiVincenzo, Norman Margolus, Peter Shor, Tycho Sleator, John A. Smolin, and Harald Weinfurter, "Elementary gates for quantum computation," Phys. Rev. A 52, 3457–3467 (1995).

[91] Michael A Nielsen and Isaac L Chuang, Quantum Computation and Quantum Information (Cambridge University Press, New York, 2000).

[92] S. Sorella, Y. Otsuka, and S. Yunoki, "Absence of a spin liquid phase in the Hubbard model on the honeycomb lattice," Sci. Rep. 2, 992 (2012).

[93] Yuichi Otsuka, Seiji Yunoki, and Sandro Sorella, "Universal quantum criticality in the metal-insulator transition of two-dimensional interacting dirac electrons," Phys. Rev. X 6, 011029 (2016).

[94] Yuichi Otsuka, Kazuhiro Seki, Sandro Sorella, and Seiji Yunoki, "Quantum criticality in the metal-superconductor transition of interacting dirac fermions on a triangular lattice," Phys. Rev. B 98, 035126 (2018).

[95] Kazuhiro Seki, Yuichi Otsuka, Seiji Yunoki, and Sandro Sorella, "Fermi-liquid ground state of interacting Dirac fermions in two dimensions," Phys. Rev. B 99, 125145 (2019).

[96] Yuichi Otsuka, Kazuhiro Seki, Sandro Sorella, and Seiji Yunoki, "Dirac electrons in the square-lattice Hubbard model with a d-wave pairing field: The chiral Heisenberg universality class revisited," Phys. Rev. B 102, 235105 (2020).

[97] Maksim Ulybyshev, Savvas Zafeiropoulos, Christopher Winterowd, and Fakher Assaad, "Bridging the gap between numerics and experiment in free standing graphene," (2021), arXiv:2104.09655 [cond-mat.str-el].

[98] Kosuke Mitarai and Keisuke Fujii, "Constructing a virtual two-qubit gate by sampling single-qubit operations," New Journal of Physics **23**, 023021 (2021).

[99] Florian Gebhard, "Gutzwiller correlated wave functions in finite dimensions d: A systematic expansion in 1/d," Phys. Rev. B **41**, 9452–9473 (1990).

[100] Kazuhiro Seki and Sandro Sorella, "Benchmark study of an auxiliary-field quantum Monte Carlo technique for the Hubbard model with shifted-discrete Hubbard-Stratonovich transformations," Phys. Rev. B **99**, 144407 (2019).

[101] Ho-Kin Tang, J. N. Leaw, J. N. B. Rodrigues, I. F. Herbut, P. Sengupta, F. F. Assaad, and S. Adam, "The role of electron-electron interactions in two-dimensional dirac fermions," Science **361**, 570–574 (2018).

[102] Seher Karakuzu, Kazuhiro Seki, and Sandro Sorella, "Solution of the sign problem for the half-filled Hubbard-Holstein model," Phys. Rev. B **98**, 201108 (2018).

[103] Natanael C. Costa, Kazuhiro Seki, Seiji Yunoki, and Sandro Sorella, "Phase diagram of the two-dimensional Hubbard-Holstein model," Communications Physics **3**, 80 (2020).

[104] Natanael C. Costa, Kazuhiro Seki, and Sandro Sorella, "Magnetism and Charge Order in the Honeycomb Lattice," Phys. Rev. Lett. **126**, 107205 (2021).

[105] Kazuhiro Seki and Seiji Yunoki, "Spatial, spin, and charge symmetry projections for a Fermi-Hubbard model on a quantum computer," Phys. Rev. A **105**, 032419 (2022).

[106] Ghassan George Batrouni and Richard T. Scalettar, "Anomalous decouplings and the fermion sign problem," Phys. Rev. B **42**, 2282–2289 (1990).

[107] Hiroyuki Shiba, "Thermodynamic Properties of the One-Dimensional Half-Filled-Band Hubbard Model. II: Application of the Grand Canonical Method," Progress of Theoretical Physics **48**, 2171–2186 (1972).

[108] Yasuhiro Hatsugai, "Quantized Berry Phases as a Local Order Parameter of a Quantum Liquid," Journal of the Physical Society of Japan **75**, 123601 (2006).

[109] Hal Tasaki, Physics and Mathematics of Quantum Many-Body Systems (Springer International Publishing, Cham, 2020) Chap. 9.

[110] Sergey B. Bravyi and Alexei Yu. Kitaev, "Fermionic quantum computation," Annals of Physics **298**, 210 – 226 (2002).

[111] Fabian H. L. Essler, Holger Frahm, Frank Göhmann, Andreas Klümper, and Vladimir E. Korepin, The One-Dimensional Hubbard Model (Cambridge University Press, New York, 2005).

[112] Frank Verstraete, J. Ignacio Cirac, and José I. Latorre, "Quantum circuits for strongly correlated quantum systems," Phys. Rev. A **79**, 032316 (2009).

[113] Thomas Barthel, Carlos Pineda, and Jens Eisert, "Contraction of fermionic operator circuits and the simulation of strongly correlated fermions," Phys. Rev. A **80**, 042333 (2009).

[114] Jun John Sakurai, Modern quantum mechanics, edited by San Fu Tuan (Benjamin-Cummings, Menlo Park, CA, 1985) Chap. 4.

[115] M. El-Batanouny and F. Wooten, "Time-reversal symmetry: color groups and the Onsager relations," in Symmetry and Condensed Matter Physics: A Computational Approach (Cambridge University Press, 2008).

[116] J. E. Hirsch, "Two-dimensional hubbard model: Numerical simulation study," Phys. Rev. B **31**, 4403–4419 (1985).

[117] Congjun Wu and Shou-Cheng Zhang, "Sufficient condition for absence of the sign problem in the fermionic quantum monte carlo algorithm," Phys. Rev. B **71**, 155115 (2005).

[118] Dong Zheng, Guang-Ming Zhang, and Congjun Wu, "Particle-hole symmetry and interaction effects in the Kane-Mele-Hubbard model," Phys. Rev. B **84**, 205121 (2011).